A DISEASE AGE STRUCTURED MODEL OF EPIDEMIC POPULATION DYNAMICS WITH PUBLIC HEALTH INTERVENTIONS

By

Xi Huo

Dissertation

Submitted to the Faculty of the

Graduate School of Vanderbilt University

in partial fulfillment of the requirements

for the degree of

DOCTOR OF PHILOSOPHY

in

Mathematics

August, 2014

Nashville, Tennessee

Approved:

Professor Glenn Webb

Professor Alexander Powell

Professor Bryan Shepherd

Professor Douglas Hardin

Professor Philip Crooke

To my dear parents,

ACKNOWLEDGMENTS

First I would like to thank my advisor, Professor Glenn Webb. I feel very fortunate to work under his supervision. Professor Webb is a great mathematician with broad interests and valuable experiences in mathematical biology. He gives me a lot of freedom on my research, and motivates me whenever I am frustrated. He always makes time for me, even during holidays. He is constantly patient in reading my work, and even patient in correcting my grammar. He has been extremely supportive on my ideas and decisions, and provided me opportunities for meeting people and presenting my work as much as he could. He has not only introduced me to the fantastic world of mathematical biology, but also guided me through the mathematical society. I am, again, very lucky to become one of his students.

I am grateful to Professor Philip Crooke for many inspiring conversations and his kind invitations to many scientific talks. I also appreciate the generous help from Dr. Mathias Wilke, in my study of differential equations and semi-group theory. I am very thankful to the other committee members, Professor Alexander Powell, Professor Bryan Shepherd, and Professor Douglas Hardin, for their agreements to become my Ph.D. committee members, and their precious time in providing comments on my articles and attending my qualifying exam and dissertation defense.

I would like to thank the mathematical biology people I meet at Vanderbilt, Cameron Browne, Georgi Kapitanov, Peter Hinow, and Zhian Wang, for being very considerate in giving me suggestions and supports. Moreover, I would like to thank the girls in the math department, Fengying, Lujun, Shiying, Sui, Wenjia, Xuemei, for growing up together in academia and spending wonderful time with me. Last but not least, many thanks to my parents and dear Ping, whose unconditional supports are my source of power.

TABLE OF CONTENTS

Page

CHAPTER I

INTRODUCTION

The work in this dissertation is about modeling the spread of an infectious disease in a closed community with two basic public health interventions: (i) identifying and isolating symptomatic cases, and (ii) tracing and quarantine of the contacts of identified infectives. Our aim is to evaluate the efficacy of tracing and quarantine strategies which are believed to be an important aspect of controlling an outbreak of emerging or re-emerging infectious diseases. The model is applicable in both emerging epidemics that require isolation, tracing, and quarantine, such as H1N1, SARS (severe acute respiratory syndrome), and influenzas, and re-emerging epidemics that requires isolation and certain vaccination strategies, such as a smallpox bioterrorist attack. Moreover, our model can be applied as a rational basis for decision makers to guide interventions and deploy public health resources in future epidemics.

I.1 Terminologies

There are two alternatives for epidemic controls, namely targeted control and mass control. Isolation of symptomatic cases is important in controlling infectious diseases, but also important is the vaccination and quarantine of traced contacts of known infectives. Contact tracing is especially important when there is a lack of rapid diagnostic methods, as was in the case of SARS Glasser et al (2011).

We next clarify the definitions of the three intervention strategies considered in the

model[1]:

1. Isolation is the process by which infected people (all of whom are symptomatic) are prevented from infecting susceptible ones.

2. Contact tracing is the process of identifying people who may have been infected by exposure to (or contact with) an infectious person.

3. Quarantine is the process of isolating these people, called contacts (none of whom is yet symptomatic, and many not even be infected).

Quarantine can be divided into two types: (i) quarantine of close contacts of identified cases, and (ii) quarantine of large groups of people (such as residents in residential complexes, workers in a workplace, students in schools, *etc*). Our model focuses on the (i) type quarantine, which is conducted as a consequence of tracing close contacts of infected individuals.

I.2 Background

There are two practical applications of our model being presented in this dissertation: (1) we assess public health guidelines about emergency preparedness and response in the event of a smallpox bioterrorist attack; (2) we simulate the 2003 SARS outbreak in Taiwan and estimate the number of cases avoided by contact tracing.

I.2.1 Smallpox

Smallpox was eradicated in 1979, but fears of bioterrorist attacks by deliberately releasing the variola virus have been taken into consideration according to federal and academic

[1]Definitions are provided by J. Glasser at Centers for Disease Control and Prevention.

observations ever since the terrorist attacks of September 11, 2001. Although the two government laboratories in the United States and Russia are the only known places that keep the viral samples, the possibility of other sources cannot be ruled out CIDRAP (2002). Public health authorities have detailed plans for emergency preparedness and response to a smallpox outbreak CDC (2003); on the other hand, the proper amount of vaccine and treatment medicine that should be stockpiled is still controversial NewYorkTimes (2013).

Due to the undesirable side-effects of the vaccine, the routine vaccination for the variola virus has been discontinued ever since 1972, and currently the vaccination is only given to selected military personnel and laboratory workers who handle the virus. Moreover, because of the waning immunity of the vaccine, the proportion of Americans who are both over age 40 and still immune to smallpox might be too small to achieve herd immunity. As a result, based on these concerns, public health authorities, such as Centers for Disease Control and Prevention (CDC), suggest intensive surveillance and identification of infected cases, isolation of smallpox patients, and vaccination of close contacts of infected individuals.

I.2.2 SARS

Distinct from smallpox, the conduct of surveillance and control strategies of modern influenzas (such as H1N1 and SARS) is less efficient due to the lack of timely vaccines, noncompliance of the public with quarantine, and the period of asymptomatic infectiousness. It is widely believed that SARS was eradicated because of limited transmission occurring before symptom onset, but the effectiveness of contact tracing is still controversial even in the regions where high levels of contact tracing were conducted, such as Taiwan and mainland China. So we apply our model to simulate the SARS outbreak in Taiwan with real data to assess the contact tracing and quarantine efficacy in avoiding infections.

I.3 Related Studies

We apply our model to assess the ring vaccination strategy in the control of smallpox, and compare the effectiveness between ring vaccination strategy and mass vaccination strategy. Various methods have been developed to evaluate public health control strategies for smallpox. Müller *et al.* investigate contact tracing by an individual based stochastic model Müller et al (2000). Meltzer *et al.* develop a Markov chain model to estimate in what levels that a combined vaccination and quarantine campaign should be taken to reduce smallpox transmission, and suggest a number of adequate vaccine doses for stockpiling Meltzer et al (2001). Halloran *et al.* construct a stochastic model to compare the effectiveness of mass vaccination versus targeted vaccination in a population of 2,000, and they conclude that targeted vaccination can prevent more cases per dose Halloran et al (2002). Eichner performs stochastic computer simulations to examine how case isolation and contact tracing prevent the spread of smallpox Eichner (2003). Kretzschmar *et al.* present a branching process stochastic model to estimate the size and duration of outbreaks contained by ring vaccination Kretzschmar et al (2004). Vidondo *et al.* approach a novel containment strategy which vaccinates "super contacts" by an individual-network based simulation Vidondo et al (2012).

There are also several ordinary differential equation (ODE) models which focus on different aspects of controlling a smallpox outbreak. Kaplan *et al.* assume a high infectivity in the prodromal period in their model with a focus on public health logistical constraints. They conclude that mass vaccination is more efficient than ring vaccination, when a congestion in the vaccination queue occurs Kaplan et al (2003), Kaplan et al (2002). Castillo-Chavez *et al.* take the behavioral changes of the community into consideration, and demonstrate that even gradual and mild changes of people's daily contact activity

can slow an epidemic Valle et al (2005). Hsieh *et al.* propose a differential equation model that includes intervention measures implemented in the control of 2003 SARS, and analyze how quarantine measures change the basic dynamics of the model Hsu and Hsieh (2006).

ODE models were used in modeling SARS as well, and in particular to investigate the impact of quarantining asymptomatic infectives Hethcote et al (2002), Wang and Ruan (2003), Hsieh et al (2004), Gumel et al (2004), Nishiura et al (2004), Fraser et al (2004), Day et al (2006), Hsu and Hsieh (2006), Arino et al (2006), Feng et al (2007), Feng et al (2009), Feng et al (2011). A thorough review of many of these works has been provided in Bauch et al (2005). The article points out that the nonlinearity of the rate of quarantining undiagnosed cases is required to be taken into account. In our work, we use a partial differential equation (PDE) model with a variable of disease age (or age since infection), with nonlinear rates of contact tracing infectives and quarantining susceptibles dependent on the rate of identifying symptomatic cases.

Although some of the previous work includes the varying levels of transmission ability and symptom scores in different disease stages, there is less work about smallpox control that takes continuous disease age into consideration. Webb *et al.* apply age structured epidemic models to investigate isolation strategy and school closings in the spread of H1N1 Webb et al (2010). Inaba *et al.* develop a series of multistate class age structured epidemic systems with isolation rate as the only intervention Inaba and Nishiura (2008). Fraser *et al.* establish an infection age-structured model that estimates the effectiveness of isolation and contact tracing in the control of epidemic diseases with a formulation different from ours Fraser et al (2004). Our model is aimed to take into consideration several key features about disease transmission and public health interventions at the same time:

(i) Continuous infection age.

(ii) Infection-age-dependent case isolation rate.

(iii) Contact tracing/quarantine/vaccination rates that depend on diagnosis rate of symptomatic cases.

(iv) Variation of susceptible population due to infection and contact tracing, quarantine, or vaccination.

CHAPTER II

PRELIMINARY: THE ODE MODEL

Before we introduce our age-structured partial differential equations model, in this chapter, we review the fundamental theory of modeling epidemic infectious disease with ordinary differential equations models. This review aims to interpret important parameters of the ODE model, as well as provide accurate understanding of the parameters in the main PDE model.

Epidemic models with ODE form a typical category of compartmental models, which divide the population into disjoint groups (compartments) based on disease status, age, or other factors. The so-called SIR model labels three compartments: S stands for the susceptible population, I is for the infected population, and R represents the recovered population. In the ODE model, the compartments are single-variable functions with respect to time. ODE and PDE models are deterministic models, in which the future states are determined by the knowledge of the present state of the system Bauch et al (2005). **?** gives a time line for the development of deterministic modeling in epidemic diseases ever since the beginning of the 20th century: Hamer (1906) formulated a discrete time model to understand the recurrence of measles epidemics, which is also the first model with the infection rate proportional to the product of the susceptible population and the infected population. Later Ross, Hudson, Martini, and Lotka developed other models to study diseases such as malaria. In 1911, Kermack and McKendrick published papers of theoretical results and formulations in epidemic models, and their models incorporated the important feature of disease age related transmission and removal rates.

II.1 Basic SIR Compartmental Model

As mentioned before, we denote $S(t)$ as the population of people who are not infected and are susceptible to the disease at time t, $I(t)$ as the population of people who are infected and infectious at time t, and $R(t)$ as the population of recovered people, who will neither infect others nor be reinfected at time t. We ignore the natural birth and death rates because the outbreak of an epidemic moves faster than the demographic rates in the population. So we have the following dynamics:

$$\begin{aligned} \frac{dS}{dt} &= -\lambda IS, \qquad S(0) = S_0 \geq 0 \\ \frac{dI}{dt} &= \lambda IS - rI, \quad I(0) = I_0 \geq 0 \\ \frac{dR}{dt} &= rI, \qquad\quad R(0) = R_0 \geq 0 \end{aligned} \tag{II.1}$$

where r is the recover rate if there is no control, and if there is a control of isolating symptomatic individuals, r can be regarded as the combination of two rates: the rate of naturally recovery without showing symptoms or being isolated, and the rate of being isolated due to showing symptoms.

In (II.1), λI is the rate of new infections (the force of infection). We denote N as the total number of people in the community, which is a constant, α as the average number of contacts one might have per unit time (per day), and β as the probability of an infected individual to transmit the disease to a susceptible person when they have contacts. For each infected individual at time t, there is a probability $S(t)/N$ to meet a susceptible person, amd there is a probability β for an infection to happen during this contact. Then each infected individual will infect $\beta \cdot S(t)/N$ susceptibles per contact, and infect $\alpha \cdot \beta \cdot S(t)/N$ susceptibles per unit time. So there will be $\alpha \cdot \beta \cdot S(t) \cdot I(t)/N$ susceptibles infected per unit time, which gives the disease infection rate.

According to the calculation above, the parameter λ in (II.1) cannot be simply understood as the disease transmission rate, it is actually a product of parameters with practical meanings: $\lambda = \alpha \cdot \beta / N$. Although a single character β has often been used to represent the infection transmission coefficient, correct understanding of the incidence rate is very important in the application.

II.2 SIR Model with Mass Control

Mass control strategies, for which a good example is the mass vaccination strategy in controlling smallpox, is a process that prevents people (both susceptible and infected) from random disease transmission, by interventions such as quarantine and vaccination. We provide the ODE model for mass control as follows (the age-structured model and background discussions are elaborated in *V*.2.1):

$$\begin{aligned} \frac{dS}{dt} &= -\lambda IS - mS, \qquad S(0) = S_0 \geq 0 \\ \frac{dI}{dt} &= \lambda IS - rI - mI, \;\; I(0) = I_0 \geq 0 \\ \frac{dR}{dt} &= rI, \qquad\qquad R(0) = R_0 \geq 0 \end{aligned} \tag{II.2}$$

where the interpretations of λ and r are the same with those in (II.1), and $m = M/N$, where M is the number of people removed due to mass control per unit time and N is the total population number. So the removal rate of susceptible population due to mass control m is interpreted as the total number of people removed by mass control per unit time, times the probability for one person being susceptible ($S(t)/N$).

II.3 SIR Model with Targeted Contact Tracing

According to targeted tracing strategies, such as contact tracing in SARS and ring vaccination in smallpox, it is reasonable to assume that the targeted tracing rate is related to the isolation rate of symptomatic individuals. In the practical control of an epidemic disease, an identified symptomatic individual will be asked to provide a list of close contacts to be traced as soon as possible. If we ignore the delay of the tracing process, then the number of people removed due to tracing will be proportionate to the number of identified cases. With this idea in mind, we have the corresponding ODE model:

$$\begin{aligned} \frac{dS}{dt} &= -\lambda IS - \kappa_s SI, \qquad S(0) = S_0 \geq 0 \\ \frac{dI}{dt} &= \lambda IS - rI - \mu I - \kappa_i I^2, \;\; I(0) = I_0 \geq 0 \\ \frac{dR}{dt} &= rI, \qquad\qquad R(0) = R_0 \geq 0 \end{aligned} \tag{II.3}$$

where in this case, λ and N are as in (II.1), r is the natural recover rate, and μ is the isolation rate of symptomatic individuals. We now interpret: $\kappa_s = \eta_s \cdot \mu \cdot C/N$, where η_s is the probability for a contact, provided by a symptomatic infective, to be susceptible, which depends on the contact tracing efficiency. C is the average number of contacts that can be effectively provided and traced per identified infective. The probability for each susceptible individual to be a contact of an identified infective is $\mu \cdot I(t)/N$. Hence the probability to be named as a traced contact is $\eta_s \cdot C$. So we have the contact tracing rates for all susceptibles as $\kappa_s I$ in (II.3). Similar interpretation applies for the contact tracing rate of infected individuals.

CHAPTER III

MAIN MODEL: AGE-STRUCTURED PDE MODEL

III.1 Notations

Before introducing the main model, we introduce the notations as follows:

(N.1) For $0 < M \leqslant \infty$, let $L^1 := L^1([0, M]; \mathbb{R})$, $L^1_+ := L^1([0, M]; \mathbb{R}_+)$ which is the positive cone in L^1. M denotes the maximum disease age in the model.

(N.2) For $0 < T \leqslant \infty$, denote $C_T := C([0, T]; L^1)$ with the supremum norm: $\|l\|_{C_T} := \sup_{0 \leqslant t \leqslant T} \|l(t)\|_{L^1}$, for $l \in C_T$. Let $C_{T,+} := C\left([0, T]; L^1_+\right)$ which is the positive cone in C_T.

The basic assumptions are as follows:

(A.1) Let $\mathcal{T} \in (L^1)^*$ with norm $\|\mathcal{T}\|_\infty$, and we assume $\mathcal{T}\left(L^1_+\right) \subseteq \mathbb{R}_+$.

(A.2) $\mathcal{B}, \mathcal{Q} : L^1 \to \mathbb{R}$ be globally Lipschitz continuous functions with Lipschitz constants $|\mathcal{B}|$ and $|\mathcal{Q}|$. Moreover, we assume $\mathcal{B}\left(L^1_+\right) \subseteq \mathbb{R}_+$ and $\mathcal{Q}\left(L^1_+\right) \subseteq \mathbb{R}_+$.

(A.3) $\mathcal{B}(0) = 0$, $\mathcal{Q}(0) = 0$.

III.2 Model

For $t \geqslant 0$, $a \in [0, M]$, the formal model is:

$$
\begin{aligned}
&\frac{\partial}{\partial t} i\left(a,t\right) \; + \frac{\partial}{\partial a} i\left(a,t\right) = \underbrace{-\mu\left(a\right) i\left(a,t\right)}_{\substack{\text{isolation of symptomatic} \\ \text{individuals with infection} \\ \text{age } a}} \underbrace{-\mathcal{T}\left(i\left(\cdot,t\right)\right) i\left(a,t\right)}_{\substack{\text{tracing of contacts} \\ \text{with infection age } a}} \\
&\frac{d}{dt} S\left(t\right) = \underbrace{-\mathcal{B}\left(i\left(\cdot,t\right)\right) S\left(t\right)}_{\text{infection of susceptibles}} \underbrace{-\mathcal{Q}\left(i\left(\cdot,t\right)\right) S\left(t\right)}_{\substack{\text{quarantine of contacts} \\ \text{that are susceptible}}} \\
&\underbrace{i\left(0,t\right)}_{\substack{\text{infectives with} \\ \text{infection age 0}}} = \underbrace{\mathcal{B}\left(i\left(\cdot,t\right)\right) S\left(t\right)}_{\text{rate of new infections}} \\
&i(a,0) = i_0(a) \in L^1\left[0,M\right] \\
&S(0) = S_0 \in \mathbb{R}_+
\end{aligned}
\tag{III.1}
$$

where $i(a,t)$ is the infected population density at infection age a at time t, and $S(t)$ is the susceptible population at time t, $\mu(a)$ is the rate of isolating symptomatic cases those are at disease age a. If we denote $i\left(\cdot,t\right)$ as the infected population density function at time t, then $\mathcal{B}\left(i\left(\cdot,t\right)\right)$ represents the infection transmission rate, $\mathcal{T}\left(i\left(\cdot,t\right)\right)$ represents the isolation rate of infected individuals due to contact tracing at time t, and $\mathcal{Q}\left(i\left(\cdot,t\right)\right)$ represents the quarantine rate of susceptible contacts as the consequence of contact tracing.

III.3 Problem Formulation

Solving for $S\left(t\right)$ from the second equation in (III.1), we can simplify the problem into an age-dependent population dynamics model for $i\left(a,t\right)$:

$$
\begin{aligned}
&\frac{\partial}{\partial t} i\left(a,t\right) \; + \frac{\partial}{\partial a} i\left(a,t\right) = -\mu\left(a\right) i\left(a,t\right) - \mathcal{T}\left(i\left(\cdot,t\right)\right) i\left(a,t\right) \\
&i\left(0,t\right) = S_0 \mathcal{B}\left(i\left(\cdot,t\right)\right) e^{-\int_0^t \mathcal{B}(i(\cdot,s))+\mathcal{Q}(i(\cdot,s))ds} \\
&i(a,0) = i_0(a)
\end{aligned}
\tag{III.2}
$$

In the following context, we denote $i\,(t)(a) := i\,(a,t)$; then $i \in C_T$ means $i(t) \in L^1$, for $t \in [0,T]$. We also refer the solutions of the age-dependent problem as $l\,(t)(a) := i\,(a,t)$, where $l \in C_T$. Next we will generalize the problem to a formulation of age-dependent population dynamics. We introduce the aging and birth functions:

(1) Let $G : L^1 \to L^1$ be the aging function.

(2) For $0 < T \leqslant \infty$, let $F : C_T = C\,([0,T]\,; L^1) \to C\,([0,T]\,; \mathbb{R})$ be the birth function.

Let $0 < T \leqslant \infty$, let $t \in [0,T]$ and $l \in C_T$, the general age-dependent problem is as follows:

$$\begin{aligned} &\frac{\partial}{\partial t} l\,(t)(a) + \frac{\partial}{\partial a} l\,(t)(a) = G(l\,(t))(a)\,,\ a.e.\ a \in [0,M] \\ &l\,(t)(0) = (F\,(l))(t) \\ &l\,(0)(a) = \phi\,(a)\,,\ a.e.\ a \in [0,M] \end{aligned} \tag{III.3}$$

However, the equation system in (III.3) is not well defined for solutions that are not continuously differentiable with respect to both variables. We are thus led to the following formulation of age-dependent population dynamics as in Webb (1985): let $0 < T \leqslant \infty$, and let $l \in C_T$ satisfy:

$$\begin{aligned} &\lim_{h \to 0^+} \int_0^M \left| h^{-1} \left[l\,(t+h)(a+h) - l\,(t)(a) \right] - G(l\,(t))(a) \right| da = 0 \\ &\lim_{h \to 0^+} \int_0^h \left| l\,(t+h)(a) - (F\,(l))(t) \right| da = 0 \\ &l\,(0)(a) = \phi\,(a)\,,\ a.e.\ a \in [0,M] \end{aligned} \tag{III.4}$$

where we let $l\,(t+h)(a+h) = 0$ if $a + h > M$.

III.4 Preliminary Results

In this section, we will present results about local existence and uniqueness of the solutions to the age-dependent problem (III.4) with the following assumptions on the aging and birth functions:

(H.1) $G : L^1 \to L^1$, there is an increasing function $c_1 : [0,\infty) \to [0,\infty)$ such that $\|G(\phi_1) - G(\phi_2)\|_{L^1} \leq c_1(r)\|\phi_1 - \phi_2\|_{L^1}$ for all $\phi_1, \phi_2 \in L^1$ such that $\|\phi_1\|_{L^1}, \|\phi_2\|_{L^1} \leq r$.

(H.2) There is a function $c_2 : [0,\infty)\times[0,\infty) \to [0,\infty)$, which is increasing and continuous w.r.t. both variables. Then for all $T > 0$, $F : C_T \to C([0,T];\mathbb{R})$, for any $0 \leq t \leq T$ and $r > 0$, we have

$$|(F(\phi_1))(t) - (F(\phi_2))(t)| \leqslant c_2(r,t) \sup_{0\leqslant s\leqslant t} \|\phi_1(s) - \phi_2(s)\|_{L^1}$$

for all ϕ_1, $\phi_2 \in C_T$ such that $\|\phi_1\|_{C_T}, \|\phi_2\|_{C_T} \leq r$.

We state theorems about local existence and uniqueness of the solutions below. The proofs (they can be found in the Appendix) are different from those in Webb (1985), since our assumption of the birth function F is different.

III.4.1 Theorem III.4.1

Theorem III.4.1. *Let (H.1) and (H.2) hold and let $\phi \in L^1$. There exists $T > 0$ and $l \in C_T$ such that l is a solution of* (III.4) *on $[0,T]$. Furthermore, there is a unique solution of* (III.4) *on $[0,T]$.*

We introduce the definition of maximal interval of existence as in Webb (1985):

III.4.2 Definition III.4.2

Definition III.4.2. Let $\phi \in L^1$. Denote $[0, T_\phi)$ as the maximal interval of existence of the solution of (III.4), is the maximal interval with the property that if $0 < T < T_\phi$, there exist $l \in C_T$ such that l is a solution of (III.4) on $[0, T]$.

With additional assumptions as stated below, we will prove the positivity of the solutions.

$(H.3)$ $F\left(C_{T,+}\right) \subseteq C\left([0,T]\,;\mathbb{R}_+\right)$

$(H.4)$ There is an increasing function $c_3 : [0,\infty) \to [0,\infty)$ such that if $r > 0$ and $\phi \in L^1_+$ with $\|\phi\|_{L^1} \leq r$, then $G(\phi) + c_3(r)\,\phi \in L^1_+$.

III.4.3 Theorem III.4.3

Theorem III.4.3. *Let (H.1)-(H.4) hold and let $\phi \in L^1_+$. The solution l of* (III.4) *on $[0, T_\phi)$, has the property that $l(t) \in L^1_+$ for $0 \leqslant t < T_\phi$.*

Furthermore, with one more restriction on the aging and birth functions, the positive solution exists globally.

III.4.4 Theorem III.4.4

Theorem III.4.4. *Let (H.1)-(H.4) hold and let $\phi \in L^1_+$, let l be the solution of* (III.4) *on $[0, T_\phi)$, and let there exist $\omega \in \mathbb{R}$ such that for $0 \leq t < T_\phi$, F and G satisfy the following inequality:*

$$(F(l))(t) + \int_0^{\mathrm{M}} G(l(t))(a)\,da \leqslant \omega \int_0^{\mathrm{M}} l(t)(a)\,da \tag{H.5}$$

Then $T_\phi = \infty$ and $\|l(t)\|_{L^1} \leq e^{\omega t}\|\phi\|_{L^1}$.

CHAPTER IV

BASIC THEORY OF THE EPIDEMIC MODEL

We will continue investigating the solutions of the specific age-dependent problem (III.2) in the sense of (III.4). First, specify the birth and aging functions:

(P.1) The aging function $G : L^1 \to L^1$ is, for $\phi \in L^1$,

$$G(\phi)(a) = -\mu(a)\,\phi(a) - \mathcal{T}(\phi)\,\phi(a).$$

(P.2) The birth function $F : C_T \to C([0,\infty];\mathbb{R})$ is, for $l \in C_T$,

$$(F(l))(t) := S_0 \mathcal{B}(l(t))\, e^{-\int_0^t \mathcal{B}(l(s))+\mathcal{Q}(l(s))ds}.$$

where μ and S_0 are as in (III.1), $\mathcal{T}$, $\mathcal{B}$, and $\mathcal{Q}$ are as in (A.1)-(A.3).

IV.1 Theorem IV.1.1

Theorem IV.1.1. *Let (A.1), (A.2) and (A.3) hold, let* $\mu \in L^\infty_+[0,\mathrm{M}]$, $S_0 > 0$, *and* $\phi \in L^1_+[0,\mathrm{M}]$. *There is a function* $l \in C\left([0,\infty);L^1_+\right)$ *such that* l *is the unique global solution of* (III.4) *with the aging function* G *and birth function* F *in (P.1) and (P.2).*

For computational convenience and the proof of the asymptotic behavior, we introduce a solution formula in the following two theorems.

IV.2 Proposition IV.2.1

Proposition IV.2.1. *Let (A.1), (A.2) and (A.3) hold, let* $\mu \in L^{\infty}_{+}[0,\mathrm{M}]$, $S_0 > 0$, *and* $\phi \in L^1_+$. *There exists* $u \in C\left([0,\infty];L^1_+\right)$ *such that* u *satisfies:*

$$u(t)(a) = \begin{cases} (\mathcal{H}(u))(t-a)\, e^{-\int_0^a \mu(b)db}, & a < t \\ \phi(a-t)\, e^{-\int_{a-t}^a \mu(b)db}, & a \geq t \end{cases} \tag{IV.1}$$

where

$$(\mathcal{H}(u))(t) = S_0\mathcal{B}\left(\frac{u(t)}{1+\int_0^t \mathcal{T}(u(s))\,ds}\right) \times \left(1+\int_0^t \mathcal{T}(u(s))\,ds\right) \times e^{-\int_0^t \mathcal{B}\left(\frac{u(s)}{1+\int_0^s \mathcal{T}(u(\tau))d\tau}\right)+\mathcal{Q}\left(\frac{u(s)}{1+\int_0^s \mathcal{T}(u(\tau))d\tau}\right)ds}$$

Moreover, u *is a solution of* (III.4) *with birth function* $\mathcal{H}$ *and aging function* $\mathcal{P}: L^1 \to L^1$, *where* $\mathcal{P}(l)(a) = -\mu(a)\, l(a)$ *for* $l \in L^1$.

IV.3 Theorem IV.3.1

Theorem IV.3.1. *Let (A.1), (A.2), and (A.3) hold, let* $\mu \in L^{\infty}_{+}[0,\mathrm{M}]$, $S_0 > 0$, *and* $\phi \in L^1_+$. *Let* $u \in C\left([0,\infty);L^1_+\right)$ *be the solution to the integral equation* (IV.1). *Then*

$$l(t)(a) = \frac{u(t)(a)}{1+\int\limits_0^t \mathcal{T}(u(\tau))d\tau} \tag{IV.2}$$

gives the unique global solution $l \in C\left([0,\infty);L^1_+\right)$ *to problem* (III.2).

By formula (IV.2), we will be able to investigate the asymptotic behaviour of the solution to (III.2) as in the next theorem. Furthermore, (IV.2) also provides a starting

point for our simulations.

IV.4 Theorem IV.4.1

Theorem IV.4.1. *Let (A.1), (A.2) and (A.3) hold, let* $\mu \in L_+^\infty [0, \mathrm{M}]$*,* $S_0 > 0$*, and* $\phi \in L_+^1$*. Assume that there is an* $a_0 \in [0, \mathrm{M})$ *such that* $\mu(a) > \mu_0 > 0$ *for all* $a \in [a_0, \mathrm{M}]$*. Then, for the unique solution of* (III.1) *in the sense of* (III.4)*,* $\lim_{t\to\infty} S(t) = S_\infty > 0$*,* $\lim_{t\to\infty} I(t) = \lim_{t\to\infty} \int_0^{\mathrm{M}} i(a,t)\, da = 0$*.*

CHAPTER V

APPLICATIONS

V.1 Parameter Interpretations

In this section, we take the ring vaccination strategy of smallpox as an example to interpret the important parameters in our model. Also known as surveillance and containment, ring vaccination consists of rapid identification, isolation, vaccination of close contacts of infected persons (primary contacts), and vaccination of contacts of the primary contact (secondary contacts). We assume that each identified individual will be asked to provide a list of contacts of an average number (denoted by CT as in the following text). Contacts that are successfully traced will be vaccinated and put under surveillance for a certain quarantine period. That is, vaccination and surveillance are follow-up procedures of tracing, and are applied to both susceptible contacts (who are in the quarantine class) and infected contacts (who are in the contact tracing class). We divide the population at time t into seven classes as shown in a flow diagram in *Fig.* V.1.

In the following context, we denote T_i as the length of the pre infectious period (infectiousness threshold), T_s as the length of the pre-symptomatic period (symptoms threshold), and F_i as the length of the infectious period. Hence $T_i + F_i$ represents the maximum disease age. We consider problem (III.1) with the same notations. Notice that the dynamics of 4 compartments illustrated in *Fig.* V.1 depend on $S(t)$ and $i\,(a,t)$, since

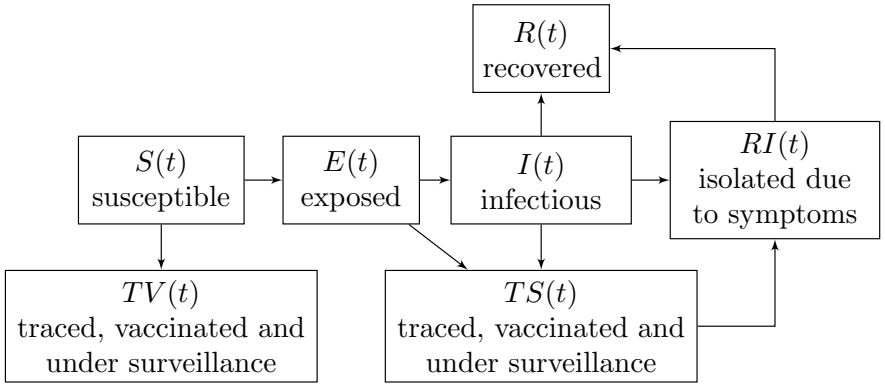

Figure V.1: Susceptible individuals may become infected, immediately enter the exposed class, $E(t)$, in which they are not yet infectious, and then enter the infectious class, $I(t)$. Symptomatic infectives in $I(t)$ may exit to the isolated class, $RI(t)$, and they will recover, enter $R(t)$, and do not return to $S(t)$ because of immunity. Susceptible people may be traced, vaccinated, put under surveillance, and they do not return to $S(t)$ because of vaccination. Exposed and infected individuals may be traced, vaccinated, put under surveillance, and then isolated when they become symptomatic. There is a possibility for infectious individuals who are neither identified due to symptoms or isolated by contact tracing, to enter class $R(t)$ when they reach the maximum disease age.

$E(t) = \int_0^{T_i} i(a,t)\,da$, $I(t) = \int_{T_i}^{T_i+F_i} i(a,t)\,da$. Moreover, we have

$$\frac{dR(t)}{dt} + \frac{dRI(t)}{dt} + \frac{dTS(t)}{dt} + \frac{dTV(t)}{dt} = \underbrace{i(T_i+F_i,t)}_{\substack{\text{recovery rate of}\\ \text{unidentified infectives}}} + \underbrace{\int_{T_s}^{T_i+F_i} \mu(a) i(a,t)da}_{\substack{\text{isolation rate of}\\ \text{symptomatic cases}}} + \underbrace{\mathcal{T}(i(\cdot,t))(E(t)+I(t))}_{\substack{\text{tracing and surveillance}\\ \text{rate of infectives}}} + \underbrace{\mathcal{Q}(i(\cdot,t))S(t)}_{\substack{\text{tracing and vaccination}\\ \text{rate of susceptibles}}}$$

Since tracing is a consequence of identifying symptomatic cases, the number of contacts traced should be related to the number of infectious cases identified. Then we assume, for simplicity, that the tracing (hence vaccinating and surveilling) rate is proportional to

the isolation (identifying new cases) rate. That is, in model (III.1), we set

$$\begin{aligned}
\mathcal{T}(i(\cdot,t)) &= \eta_I \cdot \frac{CT}{S_0} \int_{T_s}^{T_i+F_i} \mu(a)\, i(a,t)\, da \\
\mathcal{Q}(i(\cdot,t)) &= \eta_S \cdot \frac{CT}{S_0} \int_{T_s}^{T_i+F_i} \mu(a)\, i(a,t)\, da \\
\mathcal{B}(i(\cdot,t)) &= \int_{T_i}^{T_i+F_i} \beta(a)\, i(a,t)\, da
\end{aligned} \tag{V.1}$$

where $\mu(a)$ is the isolation removal rate for symptomatic infectives at disease age a as in (III.1), $\beta(a)$ is the disease transmission rate of an infectious individual at disease age a, CT is the average number of contacts provided by each identified infective, S_0 is the initial susceptible population as in (III.1), and η_I and η_S are proportionality constants for tracing the infected class and the susceptible class, respectively. Discussions about meanings and estimations of the parameters η_I and η_S are in the following context.

Contacts provided by an identified infective may come from any of the seven classes in *Fig.* V.1, but only those who are in the classes $S(t)$, $E(t)$, and $I(t)$ may be successfully traced, vaccinated, and put under surveillance. We assume that the probability for a contact being infected (or susceptible) at time t is proportional to the density of the infected (susceptible) population at time t, and we take $\eta_I(\eta_S)$ to be the constants of proportionality, respectively. Then at time t, the rate of tracing infected individuals is:

$$\underbrace{\underbrace{\eta_I \frac{E(t)+I(t)}{S_0}}_{\text{probability of tracing an infected contact}} \cdot CT}_{\substack{\text{average number of infected contacts} \\ \text{traced per identified symptomatic case}}} \cdot \underbrace{\left(\int_{T_s}^{T_i+F_i} \mu(a)\, i(a,t)\, da \right)}_{\text{rate of identifying symptomatic cases}} \tag{V.2}$$

The rate of tracing susceptible individuals is:

$$\underbrace{\underbrace{\underbrace{\eta_S \frac{S(t)}{S_0}}_{\substack{\text{probability of tracing} \\ \text{a susceptible contact}}} \cdot CT}_{\substack{\text{average number of susceptible contacts} \\ \text{traced per identified symptomatic case}}} \cdot \underbrace{\left(\int_{T_s}^{T_i+F_i} \mu(a)\, i(a,t)\, da \right)}_{\text{rate of identifying symptomatic cases}}} \tag{V.3}$$

which are exactly the corresponding terms in (III.1) with the setting (V.1). Moreover, the probability interpretations in (V.2) and (V.3) imply that for any time t, η_I and η_S should satisfy:

$$\eta_I \frac{E(t) + I(t)}{S_0} + \eta_S \frac{S(t)}{S_0} \leqslant 1 \tag{V.4}$$

We denote the probability that a traced contact of an identified symptomatic individual is infected as η, a parameter that describes the tracing efficacy in finding infectives. Hence η_I and η_S can be obtained when the value of η is given: $\eta_I = \eta \frac{S_0}{E(t)+I(t)}$ from (V.2), and $\eta_S \leqslant (1-\eta) \frac{S_0}{S(t)}$ by (V.3). Since $S(t)$ is mostly unchanged for t in the initial phase of the outbreak, for simplicity, we take $\frac{S_0}{S(t)} \approx 1$ and $\frac{S_0}{E(t)+I(t)} \approx \frac{S_0}{E(0)+I(0)}$ for any time t. So η_I and η_S are estimated by η and the initial conditions, *i.e.*, $\eta_I = \eta \frac{S_0}{E(0)+I(0)}$ and $\eta_S \leqslant 1-\eta$. The value of η can be easily determined from evolving data during the initial phase of the epidemic: it is simply the fraction of the traced contacts who turn out to be symptomatic over all traced contacts.

In particular, when $\eta_I = \eta_S = 1$, then the probability of tracing an infected contact at time t is $\eta = \frac{E(t)+I(t)}{S_0}$ and that of tracing a susceptible contact at time t is $\frac{S(t)}{S_0}$. That means the probability of tracing an infected (susceptible) contact at time t is exactly the fraction of infected (susceptible) population at time t, which indicates that the tracing is random and is not effective.

V.2 Application I: Smallpox

V.2.1 Model for Mass Vaccination

Mass vaccination, usually conducted at a constant rate, is the strategy of vaccinating large numbers of people. We assume that there is no residual immunity in the population, and a post-event mass vaccination, together with a strategy of isolating symptomatic individuals, start as soon as the first case is identified. We consider the fact that infected people vaccinated in the first few days of exposure will not transmit smallpox to others CDC (2004). And we denote T_v as the length of vaccine sensitive period for infectives, that is, infectives receive vaccination with disease age less than T_v will not be infectious. This assumption is not relevant in ring vaccination: infected contacts at any disease age are removed due to vaccination and surveillance, hence T_v is a parameter that only used in mass vaccination. *Fig.* V.2 shows the dynamic of the disease transmission with mass vaccination.

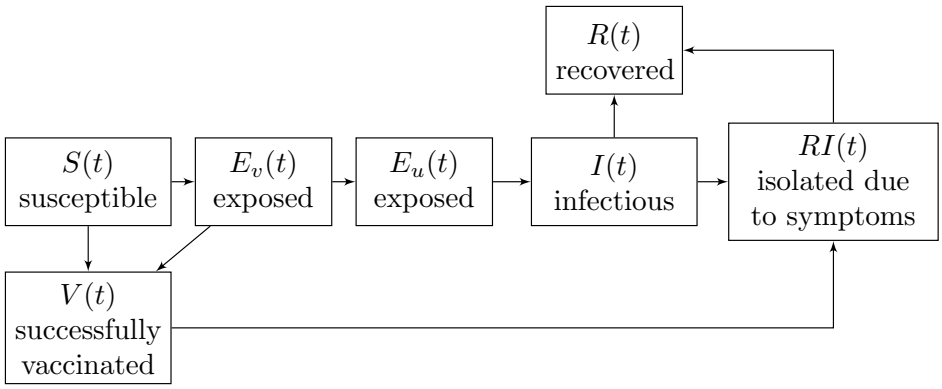

Figure V.2: $E_v(t)$ denotes the number of infectives in the vaccine sensitive stage, so they will not transmit the disease to others if vaccinated. $E_u(t)$ denotes the number of infectives in the vaccine insensitive stage, who will be able to transmit the disease even after vaccination.

Based on the dynamics stated above, we have the corresponding disease age-structured

model with mass vaccination as the only vaccination strategy that assists case isolation in (V.5). The model is of a simpler form than (III.1), which can be analyzed by the method in Webb et al (2010).

$$\begin{aligned}
&\frac{\partial}{\partial t} i(a,t) + \frac{\partial}{\partial a} i(a,t) = -\mu(a)\, i(a,t) - \nu(a)\, i(a,t),\ 0 \leqslant a \leqslant T_i + F_i,\ t \geqslant 0 \\
&\frac{d}{dt} S(t) = -\left(\int_{T_i}^{T_i+F_i} \beta(a)\, i(a,t)\, da \right) S(t) - \nu_0 S(t),\ t \geqslant 0 \\
&i(0,t) = \left(\int_{T_i}^{T_i+F_i} \beta(a)\, i(a,t)\, da \right) S(t),\ t \geqslant 0 \\
&i(a,0) = i_0(a),\ 0 \leqslant a \leqslant T_i + F_i,\ S(0) = S_0
\end{aligned} \tag{V.5}$$

where $\nu(a)$ is the mass vaccination removal rate of infected individuals at disease age a, ν_0 is the mass vaccination rate, and the other notations have the same interpretations as in the ring vaccination model. We can express different disease stages in *Figure* V.2 in terms of the infected population density function as: $E_v(t) = \int_0^{T_v} i(a,t)\, da$, $E_u(t) = \int_{T_v}^{T_i} i(a,t)\, da$, and $I(t) = \int_{T_i}^{T_i+F_i} i(a,t)\, da$.

V.2.2 Model Parameters

Table 1 describes smallpox natural history and *Table 2* shows parameter values/ranges we choose for simulations. We pick the threshold values of T_i, T_s and F_i as recommended in Eichner (2003) and CDC (2004). *Fig.* V.3a illustrates the transmission rate function of disease age, the shape of the function suggested in studies Aldis and Roberts (2005), Carrat et al (2008), Eichner (2003), CDC (2004), and Valle et al (2005), and we make a theoretical estimation about the value of the transmission rate. We vary R_{sym}, the percentage of symptomatic individuals removed per day, from 50% to 90%, which is an estimation of an efficient removal process of smallpox due to its identifiable symptoms after the prodrome.

We model a deliberate release of smallpox pathogen in a big city as large as New York, which has a total population of 8×10^6. All of the simulations start with an age distribution of index cases as shown in *Fig.* V.3b, which corresponds to a scenario when one or several public places encounter a series of smallpox virus releases.

Table 1. Smallpox durations of the progression stages.

Stage	Duration	Infectiousness	References
Incubation period	$7 \sim 17$ days	Not infectious	CDC (2004)
Initial symptoms(prodrome)	$2 \sim 4$ days	Sometimes infectious	CDC (2004)
Early rash	4 days	Most infectious	CDC (2004)
Pustular rash and scabs	16 days	Infectious	CDC (2004)
Scabs resolved		Not infectious	CDC (2004)

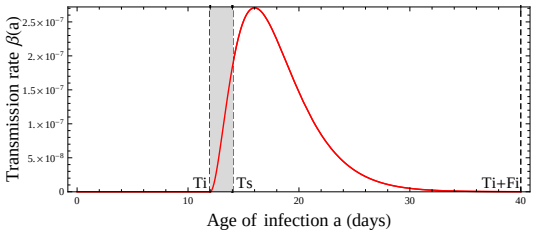

(a) Infection transmission rate function β

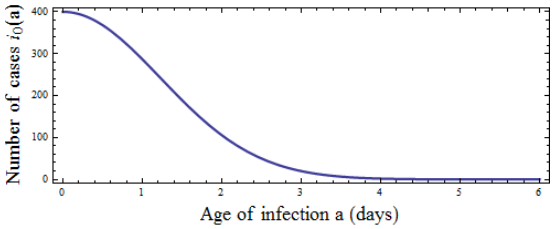

(b) Initial disease-age distribution function i_0

Figure V.3: *Fig.* V.3a is the infection age-dependent transmission rate function with respect to age since infection. T_i, T_s, and F_i are introduced and estimated as in the context and *Table 2.* The grey area is the prodromal period with initial symptoms and early contagiousness. *Fig.* V.3b is the initial disease distribution function i_0.

V.2.3 Simulations of Different Vaccination Strategies: Mass Vaccination versus Ring Vaccination

There are two ring vaccination scenarios in *Fig.* V.4: the green curves represent an effective ring vaccination strategy, and the blue curves represent an ineffective ring vaccination strategy when $\eta_I = \eta_S = 1$. We observe pulses in the daily number of traced and vaccinated contacts in both of the two scenarios. These pulses are caused by the choice of the

Tale 2. Baseline parameters and initial conditions.

Parameter description	Parameter baseline value	References
infectiousness threshold	$T_i = 12$ days	Eichner (2003)
symptoms threshold	$T_s = 14$ days	CDC (2004), Eichner (2003)
vaccine insensitiveness threshold†	$T_v = 3$ days	CDC (2004)
length of infectious period	$F_i = 28$ days	CDC (2004)
infection transmission rate function	$\beta(a) = \begin{cases} 0, & 0 \leqslant a < 12 \\ 2.5 \cdot 10^{-8}(a-12)^2 e^{-0.5(a-12)}, & 12 \leqslant a \leqslant 40 \end{cases}$	*Fig.* V.3a
removal of symptomatic cases	$R_{sym} \geqslant 50\%$ per day	Webb et al (2010), Meltzer et al (2001)
isolation rate of infectives	$\mu(a) = \begin{cases} 0.0, & a \leqslant 14 \\ -\ln(1.0 - R_{sym}), a > 14 \end{cases}$	Webb et al (2010)
mass vaccination removal rate of infectives†	$\nu(a) = \begin{cases} \nu_0, \ 0 \leqslant a \leqslant 3 \\ 0, \ a > 3 \end{cases}$	CDC (2004)
mass vaccination rate†	$0 \leqslant \nu_0 \leqslant 10000$	Kaplan et al (2003)
average number of contacts traced per identified case*	$0 < CT \leqslant 100$	Kaplan et al (2003)
probability for a traced contact being infected*	$0 < \eta \leqslant 1$	Text
initial susceptible population	$S_0 = 8 \times 10^6$	Text
index cases distribution	$i_0 \in L^1_+[0, T_i + F_i]$	*Fig.* V.3b

*parameters only used in ring vaccination.
†parameters only used in mass vaccination.

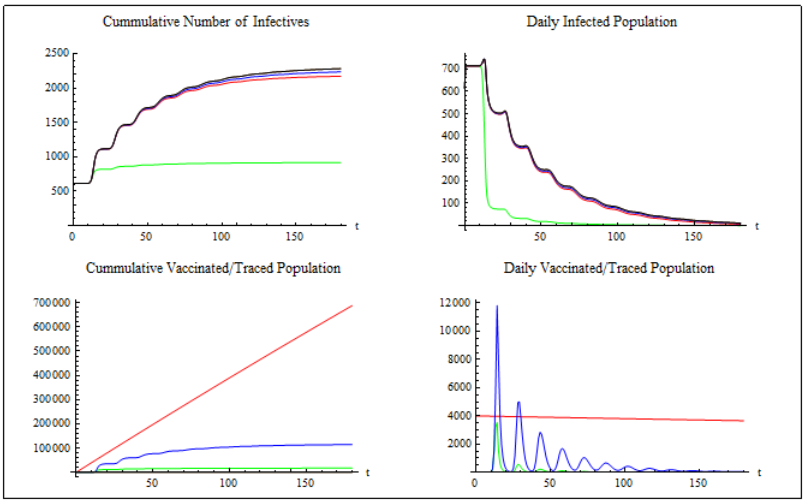

Figure V.4: There are four different cases included in this figure. The green curves stand for the case with effective ring vaccination when $CT = 50$, $R_{sym} = 50\%$, and $\eta = 0.1$. The blue curves represent the case with ineffective ring vaccination when $CT = 50$, $R_{sym} = 50\%$, and $\eta_I = \eta_S = 1$, so $\eta = \frac{I(t)+E(t)}{S_0}$. The red curves are for the case with mass vaccination when $R_{sym} = 50\%$ and the mass vaccination rate is 4000 individuals per day. The black curves correspond to the case with an isolation removal rate of $R_{sym} = 50\%$ but no vaccination.

initial infection-age distribution function in *Fig.* V.3b. The majority of the index cases are in an early disease age, and thus they will become infectious and symptomatic in the same time period. As a consequence, symptomatic cases and generations of new cases will appear as pulses; hence daily traced contacts will appear as pulses, since the tracing rate depends on the isolation rate of symptomatic cases.

Fig. V.4 also gives comparison between ring and mass vaccination strategies from different aspects: (1) the effective ring vaccination strategy prevents the most cases from occurring and requires less personnel and less vaccine stockpiles; (2) the effective ring vaccination strategy does not require a large number of people to be traced everyday, and is more efficient in controlling the outbreak compared to the mass vaccination (red curves), which requires vaccination of a large number of people everyday; (3) the ineffective ring

vaccination has similar results in controlling the outbreak as the mass vaccination (red curves), even though it consumes less vaccine stockpiles in total; it requires extremely heavy daily contact tracing load at times; (4) compared with the case of no vaccination (black curves), mass vaccination and ineffective ring vaccination prevent hundreds of cases from happening; (5) further simulations show that, for higher R_{sym} values, non-vaccination could control the spread of smallpox as well as mass vaccination and ineffective ring vaccination, while in contrast effective ring vaccination attains significant improvement in reducing total number of cases.

We also take into consideration the fact that tracing, vaccinating, and surveilling a contact in ring vaccination demands a different level of personnel effort than in mass vaccination. So in *Fig.* V.5, we compare an effective ring vaccination of a highest daily contact tracing rate of $4,000$ contacts per day, with a mass vaccination of a constant daily vaccination rate of $12,000$ people per day. That is, we assume that tracing, vaccinating, and surveilling a contact requires three times more effort than the comparable mass vaccination effort. As can be seen from the simulation, the effective ring vaccination prevents more cases, and vaccinates less people than the mass vaccination, which would also help reduce serious vaccination side effects.

V.2.4 Simulations of Ring Vaccination: Assessing Impacts of Parameters

In order to provide guidance to public health authorities for containment and surveillance strategies, we vary the three variables, CT, η, and R_{sym}, to assess different levels of ring vaccination by evaluating: (1) total number of infected cases, and (2) the percentage of traced individuals.

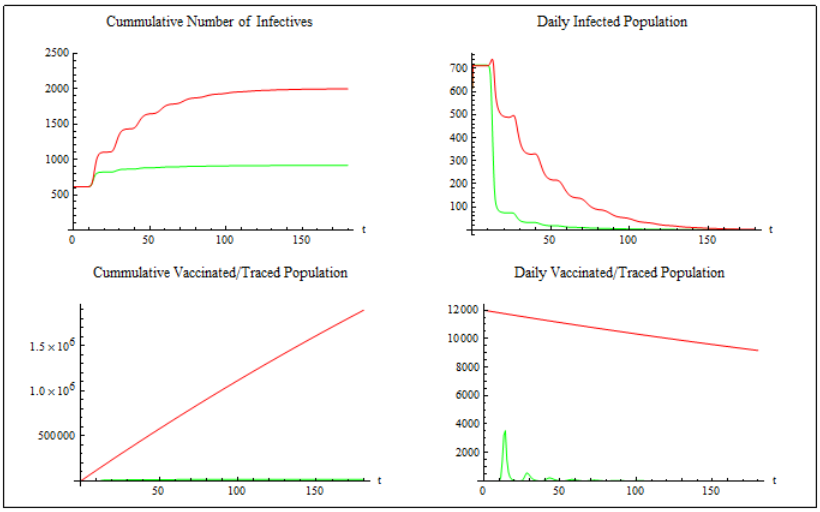

Figure V.5: The green curves stand for the case of an effective ring vaccination when $CT = 50$, $R_{sym} = 50\%$, and $\eta = 0.1$. The red curves are for the case of mass vaccination when $R_{sym} = 50\%$ and the mass vaccination rate is $1,2000$ individuals per day.

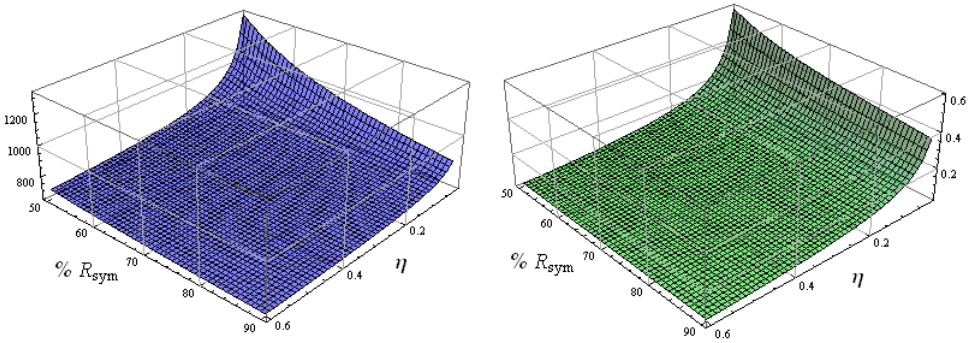

total number of cases % of people traced

Figure V.6: The blue surface is the total number of cases as a function of daily removal percentage of symptomatic cases $50\% \leqslant R_{sym} \leqslant 90\%$, and the probability that a traced contact of an identified symptomatic individual is infected $0 < \eta \leqslant 0.6$. The number of contacts traced per identified case is $CT = 50$. The green surface is the percentage of contact traced individuals as a function of the same variables under the same settings.

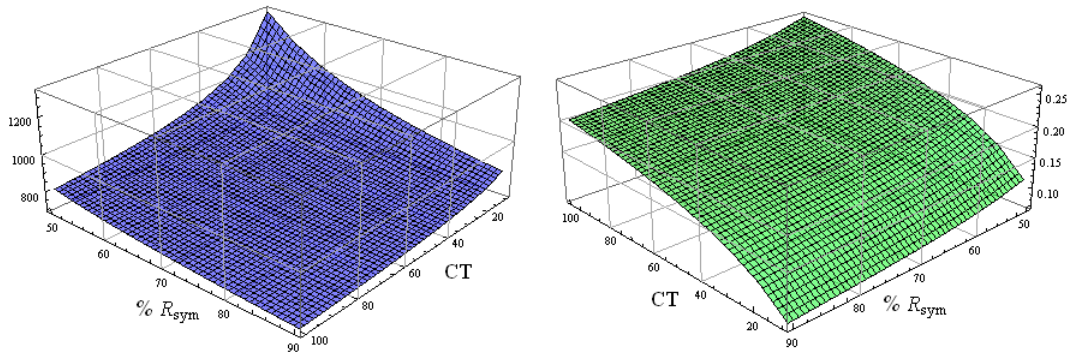

total number of cases % of people traced

Figure V.7: The blue surface is total number of infected cases as a function of daily removal percentage of symptomatic cases $50\% \leqslant R_{sym} \leqslant 90\%$, and the average number of contacts traced per identified case $10 \leqslant CT \leqslant 100$. The probability for tracing an infected contact is fixed as we take $\eta = 0.1$. The green surface is the percentage of contact traced population as a function of the same variables under the same settings.

The simulation results in *Fig.* V.6 are intuitively reasonable: for fixed $CT = 50$, high efficacies of both isolation and contact tracing will prevent more cases and save more personnel engaged in tracing. Increasing η enables us to trace more infected contacts per identified case, and it in turn saves personnel efforts. When the values of η and R_{sym} are relatively small, increasing either one of them is efficient in both controlling the outbreak and relieving the burden of tracing. If we are already able to maintain the isolation and contact tracing at a relatively high level, increasing either of the two levels would require more personnel to be involved, but just improve the results slightly.

We fix $\eta = 0.1$ in *Fig.* V.7, and notice that raising the value of CT does help reduce the total number of cases, but it also boosts the demand for the number of health care workers engaged in tracing, vaccinating, and surveilling. For fixed value of η, increasing CT helps reduce infections in two ways: increasing the number of infected contacts traced per identified case; and increasing the number of susceptible contacts quarantined which

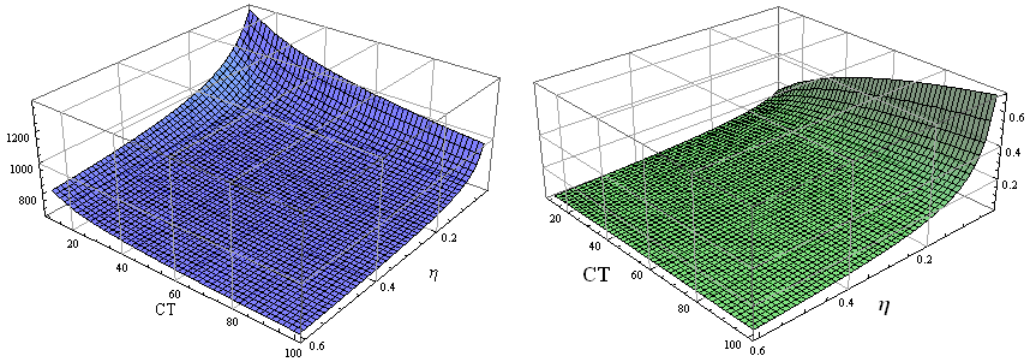

total number of cases % of people traced

Figure V.8: The blue surface is attack ratio as a function of the probability that a traced contact of an identified symptomatic individual is infected $0 < \eta \leqslant 0.6$, and the number of contacts traced per identified case $10 \leqslant CT \leqslant 100$. The daily removal percentage of symptomatic cases is fixed as $R_{sym} = 60\%$. The green surface is the percentage of contact traced population as a function of the same variables under the same settings.

results in lower infection rates. Since large values of CT and R_{sym} require more public health resources, it is left to the public health officials to determine appropriate levels of contact tracing and isolation. In the case when an effective vaccination is absent, we do not expect to quarantine a great amount of susceptibles, so the decision of increasing CT should be carefully made.

In *Fig.* V.8, we assume that the removal percentage of symptomatic cases is fixed as 60%. CT and η represent different aspects of ring vaccination strategy, and this simulation suggests how to deploy resources assigned in tracing and control the outbreak in a more economical way. In contrast to *Fig.* V.7, when contact tracing is of higher efficacy in finding infected contacts, increasing the average number of contacts provided by each identified symptomatic case does not boost greatly the demand for personnel and vaccine stockpiles. So under the assumption that the tracing efficiency η can be maintained while

CT is increased, tracing more contacts per case will help prevent cases and will not result in much more tracing work.

V.3 Application II: Influenzas: SARS

In this section, we apply our model to investigate contact tracing effectiveness in control of modern influenzas and take the outbreak of SARS as an example. First, we use our model to simulate the SARS outbreak in Taiwan, 2003 by real data. Then we modify the length of presymptomatic period hypothetically in order to provide suggestions about the efficacy of contact tracing under different circumstances. We apply our model to simulate the SARS outbreak in Taiwan, 2003, concentrated in the Taipei-Keelung metropolitan area (with a population of 6 million in 2003), because of the extensive available data and the high efficiency of contact tracing in Taiwan.

V.3.1 Parameters

In *Table 3*, we list the parameters that are obtained from real data MMWR (2003) and clinical studies of SARS. In MMWR (2003), we count the total number of traced close contacts as $12,394$. Of those there are only 33 confirmed to be infected. In this way we set $\eta \approx 33/12394$ and $CT \approx 12394/300$, where 300 is approximately the total number of cases in Taipei-Keelung metropolitan area (which we refer to Taipei area for short in the following context). The setting of the baseline values has three uncertain aspects: (1) $T_s - T_i$ determines the length of the incubation period: we set that to be 1.0 day in the data fitting in subsection 6.2. (2) We make an assumption of the shape of transmission rate function β based on laboratory diagnosis of SARS Carrat et al (2008), Peiris and *et al.* (2003), Chan and *et al.* (2004), and determine its value by estimating the basic

reproduction number of SARS in Taiwan as about 4.8 Hsieh et al (2004), Bauch et al (2005). (3) We estimate the shape of the removal rate function of symptomatic individuals μ by comparing it to studies Gumel et al (2004), Nishiura et al (2004), Carrat et al (2008). We estimate the maximal value of μ in *Fig.* V.9b by fitting data of SARS in the Taipei area.

Table 3. Baseline Parameters

Parameter description	Baseline values	References
infectiousness threshold	$T_i = 5.0$ days	Meltzer (2004), Hsu and *et al.* (2003)
symptoms threshold	$T_s = 6.0$ days	Meltzer (2004), Hsu and *et al.* (2003)
length of infectious period	$F_i = 21.0$ days	Meltzer (2004), Hsu and *et al.* (2003)
isolation rate of infectives	*Fig.* V.9b	Gumel et al (2004), Nishiura et al (2004)
infection transmission rate function	*Fig.* V.9a	Hsieh et al (2004), Bauch et al (2005), Carrat et al (2008), Peiris and *et al.* (2003), Chan and *et al.* (2004)
average number of contacts traced per identified case	$CT \approx 12394/300$	MMWR (2003)
probability for a traced contact being infected	$\eta \approx 33/12394$	MMWR (2003)
initial susceptible population	$S_0 = 6 \times 10^6$	Text
index cases distribution	*Fig.* V.9c	Hsieh et al (2004), MMWR (2003)

V.3.2 Data Fitting

Our simulation results are shown in *Fig.* V.10. Compared to simply using isolation of symptomatic cases, enforced contact tracing can help prevent 40 individuals from being infected. That means contact tracing and quarantine of more than $12,000$ people in the

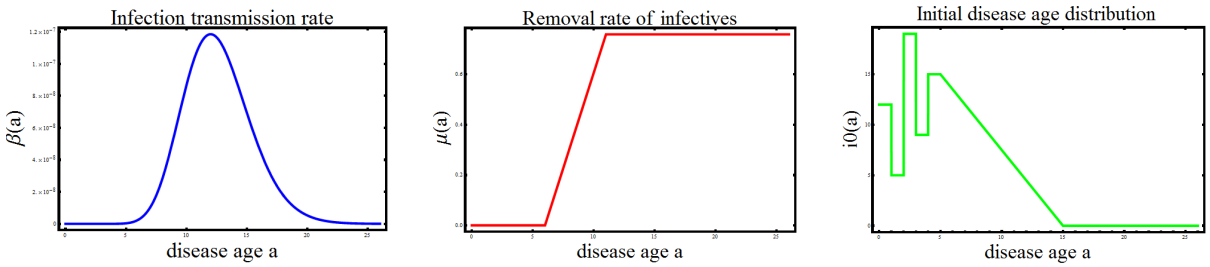

(a) Infection transmission rate function β **(b)** Removal rate function μ **(c)** Initial disease age distribution i_0

Figure V.9: The β, μ, and i_0 functions we use to fit the SARS data in Taiwan, 2003.

Taipei area enabled public health officials to discover 33 infected cases, and thus about 7 cases were avoided.

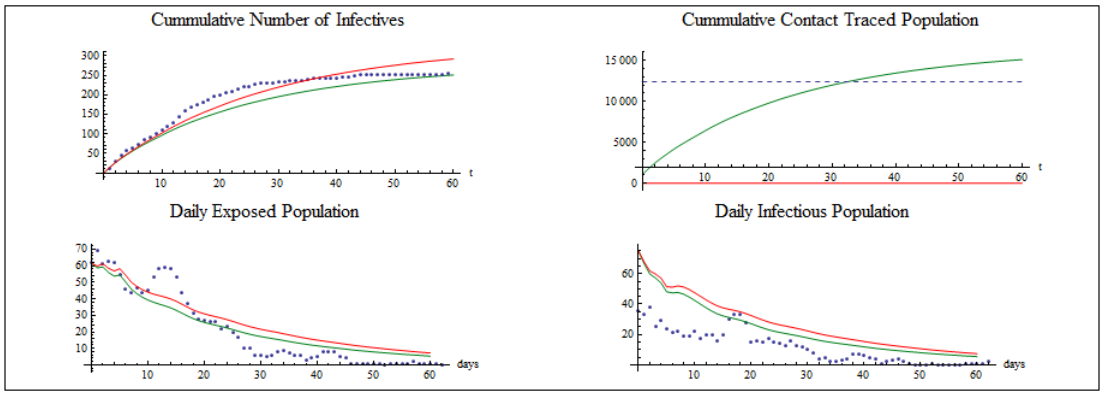

Figure V.10: The blue dots are the real data from the SARS outbreak in Taipei-Keelung metropolitan area, 2003. The green curves represent our simulation to fit the real data with parameters in *Table 3*. The red curves stand for the assumption that there is only isolation of symptomatic cases but no contact tracing implemented.

V.3.3 Alternative Fitting Parameters

In *Fig.* V.11, we modify two of the uncertain parameters mentioned before, the length of presymptomatic period $T_s - T_i$ and the removal rate of symptomatic infectives (which is the highest value of the removal rate function μ), and fit the data from Taiwan SARS.

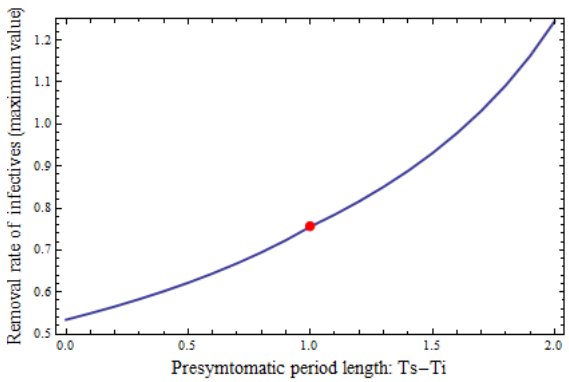

Figure V.11: The blue curve stands for pairs of parameters, incubation period length $T_s - T_i$ and maximum removal rate of symptomatic infectives, that can be applied in our model in order to fit the outbreak data of SARS, Taipei area. The red dot is the pair of parameter we used in the data fitting *Fig.* V.10. Further simulation indicates that the number of cases that are avoided by contact tracing remains the same no matter which pair of the parameters we take.

As can be inferred from *Fig.* V.11, longer incubation period requires higher efficiency of symptomatic case isolation in order to maintain the total number of cases at the same level. As a consequent result, we observe that the number of cases that are avoided by contact tracing under all pairs of parameters in *Fig.* V.11 is as much as 40. Which means, we can assess the effectiveness of contact tracing in SARS, Taiwan without an accurate estimation of the incubation period since different assumptions lead to similar results.

CHAPTER VI

DISCUSSIONS AND FUTURE WORK

We have introduced a general epidemic model that takes age since infection into consideration, to model interventions such as contact tracing, quarantine, and vaccination. Our model is applicable to different control strategies that can be formulated consistent with the hypotheses $(A.1) - (A.3)$. The global existence, uniqueness, and asymptotic behaviour of solutions are proved in the appendix. The theoretical results in Section 3 are true for non-linear age-dependent models with aging and birth functions satisfying (H.1) and (H.2), where (H.2) applies to different conditions than that in Webb (1985). Compared to previous models with infection age as a continuous variable, we are able to incorporate some important aspects of the spread and control of an epidemic disease in the model, together with practical interpretations of the corresponding parameters. For example, (i) by considering the simplified fact that the tracing rate varies according to case identification rate, we will be able to understand one of the reasons for small fluctuations that usually appear in daily cases in many of the real data; (ii) decrease of susceptible population due to public health interventions is not negligible when the interventions successfully protect a considerable amount of people from infection.

In application I, we use our model to assess public health guidelines in the event of a smallpox bioterrorist attack in a large urban center. Our simulation falls into the scenario that releases of the virus take place in the community with people being unaware of them. But we can easily modify the initial conditions to simulate other initial scenarios, such as when index cases are introduced into the community by a smallpox release in

another area, while the government and the public are getting prepared and in a watchful state. Our simulation results point out that with a limited amount of vaccine stockpiles and healthcare workers, ring vaccination is more efficient in preventing the disease from spreading than mass vaccination. With the initial condition in *Fig.* V.3b, there are not many people in the vaccination queue at the beginning of the outbreak. In this case, ring vaccination allows the early vaccine distribution for selected groups to enhance the response readiness CDC (2003), and hence allows more efficient utilization of vaccination capacity.

We also investigate the ring vaccination effectiveness by varying the three key parameters: isolation rate, contacts traced per case, and contact tracing efficiency in finding infectives. *Fig.* V.6 and *Fig.* V.7 also confirm the conclusion in Day et al (2006): tracing and quarantine help avert more cases when the isolation of symptomatic cases is ineffective. Additionally, we show that in the case of smallpox, the effectiveness of ring vaccination in reducing infections increases *at an accelerating rate as the effectiveness of isolation diminishes*[1] when the ring vaccination efficacy is of a normal level, but it increases at an almost constant lower rate when the ring vaccination efficacy is of a higher level.

Our model is able to provide guidance to public health decisions to adjust current contact tracing strategies either before or during an outbreak with updated data. All the parameters in our model have good epidemiological interpretations and are easy to estimate with data from historical epidemic outbreaks. Unlike many other studies, we take into consideration susceptible population variation due to quarantine and vaccina-

[1]Quote from Day et al (2006)

tion, which usually leads to community herd immunity. So when vaccines are available, our model can be applied to provide guidelines for vaccination strategies to create herd immunity[2].

In application II, we show that our simulation of SARS in Taiwan fits well with the observed data, and we are able to answer the question about how many cases are avoided by implementing contact tracing and quarantine in the control of the outbreak. With more precise data about each identified case, we would be able to estimate the case isolation rate accurately, and our model would enable us to determine the length of incubation period by data fitting. Therefore, our model would also be helpful in estimating important parameters and predicting transmission dynamics with evolving data during an outbreak. A great difference between the two applications we present in the paper is, contact tracing applied to control SARS in Taiwan, 2003 is not as effective as ring vaccination strategy in eradicating smallpox. The theoretical reason is that we have different settings of contact tracing parameters CT, η_I, and η_S in the two applications. In reality, our settings are quite reasonable due to facts such as the severity of symptoms, availability of vaccines (since vaccination is an important way to create herd immunity), and readiness of the public health officials with the preparedness and containment plans.

Our simulations can guide public health officials in adjusting levels of different strategies to control the outbreak and deploy resources efficiently. With theoretical suggestions, realistic adjustments about how to deploy limited resources (such as vaccine stockpiles, healthcare workers, surveillance stations, *etc.*) to meet the theoretical levels would strongly depend on the decisions of public health authorities. Furthermore, with cost-

[2]A historical example is the "ring" vaccination strategy used to eliminate smallpox

effectiveness data, we can apply optimal control methods to quantitatively determine the best control strategies.

Furthermore, the age-structured model possesses great potential in modeling the vaccination strategy of HIV (although the HIV vaccine does not exist so far, several encouraging studies such as Hansen and *et al.* (2013) suggest that there is a significant hope in the future). The HIV infection has an extremely long asymptomatic period and many HIV-positive people are unaware of their infection with the virus. Thus, an active infected individual would spread the disease without even being aware of the infection, which makes the control and detection of HIV very difficult. Even though we might have an HIV vaccine available in the future, with possible serious side-effects, it might be too limited and costly to be available to everyone at the beginning. So the deployment of a limited amount of vaccine will be a serious issue. Then, because of the prolonged asymptomatic stage of HIV infection, the effects of certain intervention strategies would depend even more on the age of infection. Our model will be an advantageous starting point for such investigation.

CHAPTER VII

PROOFS OF THE THEORETICAL RESULTS

VII.1 Theorem III.4.1

Theorem III.4.1 can be proved by the following three propositions:

Proposition VII.1.1. *Let (H.1), (H.2) hold, let $T > 0$, let $\phi \in L^1$, and let $l \in C_T$. If l is a solution of the integral equation:*

$$l(t)(a) = \begin{cases} (F(l))(t-a) + \int_{t-a}^{t} G(l(s))(s+a-t)\,ds, & 0 < a < t \\ \phi(a-t) + \int_{0}^{t} G(l(s))(s+a-t)\,ds, & t \le a \le \mathrm{M} \end{cases} \tag{VII.1}$$

on $[0,T]$, then l is a solution of (III.4) *on $[0,T]$.*

Proof. The proof is similar to that of Proposition 2.1 in Webb (1985), except that we can use the uniform continuity of the function $t \mapsto (F(l))(t)$ from $[0,T]$ to $\mathbb{R}$ for $l \in C_T$ instead in this proof. □

Proposition VII.1.2. *Let (H.1), (H.2) hold and let $r > 0$. There exists $T > 0$ such that if $\phi \in L^1$ and $\|\phi\|_{L^1} \le r$, then there is a unique function $l \in C_T$ such that l is a solution of* (VII.1) *on $[0,T]$.*

Proof. We will prove it by contraction mapping theorem. We fix $r \geqslant \|\phi\|_{L^1} > 0$ and choose $T > 0$ such that

$$T \cdot \left[c_1(2r) + c_2(2r,T) + \frac{\sup_{0\le t\le T} |(F(0))(t)| + \|G(0)\|_{L^1}}{2r} \right] \le \frac{1}{2}$$

Then define S as a closed subset of C_T:

$$S := \left\{ l \in C_T : l(0) = \phi,\ \|l\|_{C_T} \leq 2r \right\}$$

We define a mapping K on S as following and prove that K is a strict contraction from S into S.

$$(K(l))(t)(a) = \begin{cases} (F(l))(t-a) + \int_{t-a}^{t} G(l(s))(s+a-t)\,ds,\ a.e.\, a \in (0,t) \\ \phi(a-t) + \int_{0}^{t} G(l(s))(s+a-t)\,ds,\ a.e.\, a \in [t, M] \end{cases}$$

we need to verify that the following conditions hold:

(i) Let $l \in S$, $t \in [0,T]$, then $\|(K(l))(t)\|_{L^1} \leqslant 2r$.

(ii) Let $l \in S$ and let $0 \leq t < \hat{t} \leq T$, then $\left\|(K(l))(t) - (K(l))\left(\hat{t}\right)\right\|_{L^1} \to 0$ as $\left|\hat{t} - t\right| \to 0$.

(iii) Let l_1, $l_2 \in S$, then $\|K(l_1) - K(l_2)\|_{C_T} \leq \frac{1}{2}\|l_1 - l_2\|_{C_T}$.

For (i), we will only consider the case when $0 \leq t \leq \min\{M, T\}$. (Otherwise, we have

$t \geqslant M \geqslant a$, then we just need to consider the expression of $(K(l))(t)(a)$ for $a \in (0,t)$.)

$$
\begin{aligned}
&\|(K(l))(t)\|_{L^1} = \int_0^M |(K(l))(t)(a)|\,da \\
\leqslant &\int_0^t \left|(F(l))(t-a) + \int_{t-a}^t G(l(s))(s+a-t)\,ds\right| da \\
&+ \int_t^M \left|\phi(a-t) + \int_0^t G(l(s))(s+a-t)\,ds\right| da \\
\leqslant &\int_0^t |(F(l))(s)|\,ds + \int_0^{M-t} |\phi(s)|\,ds + \int_0^t \int_{t-s}^M |G(l(s))(s+a-t)|\,dads \\
\leqslant &\int_0^t |(F(l))(s) - (F(0))(s)|\,ds + \int_0^t |(F(0))(s)|\,ds + \int_0^M |\phi(s)|\,ds \\
&+ \int_0^t \|G(l(s)) - G(0)\|_{L^1} ds + \int_0^t \|G(0)\|_{L^1} ds \\
\leqslant &c_2(2r,t)\int_0^t \sup_{0\leqslant\tau\leqslant s} \|l(\tau)\|_{L^1} ds + t\cdot \sup_{0\leqslant s\leqslant t} |(F(0))(s)| + \|\phi\|_{L^1} \\
&+ c_1(2r)\int_0^t \|l(s)\|_{L^1} ds + t\cdot\|G(0)\|_{L^1} \\
\leq &2rT\left[c_1(2r) + c_2(2r,T) + \frac{\sup\limits_{0\leq t\leq T} |(F(0))(t)| + \|G(0)\|_{L^1}}{2r}\right] + r \leq 2r
\end{aligned}
$$

For (ii), we can just follow the same estimation in the proof of Proposition 2.2 in Webb (1985), except that we need to use the uniform continuity of the function $t \mapsto (F(l))(t)$ from $[0,T]$ to $\mathbb{R}$ for $l \in C_T$. (i) and (ii) imply that K maps S into S, (iii) shows that K is a contraction.

To prove (iii), given any l_1, $l_2 \in S$, we consider $0 \leq t \leq \min\{M, T\}$. Similarly we have:

$$\begin{aligned}
&\int_0^M \left|\left(K\left(l_1\right)\right)(t)(a) - \left(K\left(l_2\right)\right)(t)(a)\right| da \\
\leq &\int_0^t \left|\left(F\left(l_1\right)\right)(s) - \left(F\left(l_2\right)\right)(s)\right| ds + \int_0^t \left\|G\left(l_1(s)\right) - G\left(l_2(s)\right)\right\|_{L^1} ds \\
\leq &\int_0^t c_2(2r, s) \sup_{0 \leqslant \tau \leqslant s} \left\|l_1(\tau) - l_2(\tau)\right\|_{L^1} ds + c_1(2r) \int_0^t \left\|l_1(s) - l_2(s)\right\|_{L^1} ds \\
\leq &T \cdot \left[c_1(2r) + c_2(2r, T)\right] \left\|l_1 - l_2\right\|_{C_T} \leq \frac{1}{2} \left\|l_1 - l_2\right\|_{C_T}
\end{aligned}$$

□

Proposition VII.1.3. *Let (H.1), (H.2) hold, let $\phi, \hat{\phi} \in L^1$, let $T > 0$, and let $l, \hat{l} \in C_T$ such that l, $\hat{l}$ is the solution of* (III.4) *on $[0, T]$ for ϕ, $\hat{\phi}$, respectively. Let $r > 0$ such that $\|l\|_{C_T}, \left\|\hat{l}\right\|_{C_T} \leq r$. Then for $0 \leq t \leq T$,*

$$\left\|l(t) - \hat{l}(t)\right\|_{L^1} \leqslant e^{[c_1(r) + c_2(r,T)]t} \left\|\phi - \hat{\phi}\right\|_{L^1}$$

Hence we have the uniqueness of the local solution of (III.4).

Proof. For each $t \in [0, T]$ we define two continuous functions:

(1) $V(t) := \left\|l(t) - \hat{l}(t)\right\|_{L^1} = \int_{-t}^{M-t} \left|l(t)(t + c) - \hat{l}(t)(t + c)\right| dc$

(2) $W(t) := \sup_{0 \leqslant s \leqslant t} \left\|l(s) - \hat{l}(s)\right\|_{L^1} = \sup_{0 \leqslant s \leqslant t} V(s)$

Next, we estimate $\limsup_{h \to 0^+} h^{-1} \left[W(t + h) - W(t)\right]$ for each fixed $t \in [0, T]$ separately under the following two situations:

(i) $V(t) < W(t)$ (as shown in *Fig.* VII.1), i.e., $\exists t_0 < t$ such that $W(t) = V(t_0) > V(t)$. Since the mapping $s \mapsto V(s)$ is continuous, we can choose sufficiently small $h > 0$

such that $V(t+\delta) \leqslant V(t_0)$ for $0 \leqslant \delta \leqslant h$, hence $W(t+\delta) = W(t)$ for $0 \leqslant \delta \leqslant h$. Then $\limsup_{h \to 0^+} h^{-1} [W(t+h) - W(t)] = 0$.

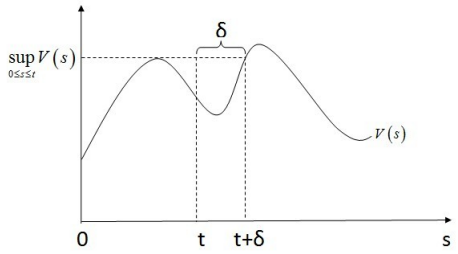

Figure VII.1

(ii) $V(t) = W(t)$, i.e., the function V attains the supremum value in $[0, t]$ at t. Then we have

$$
\begin{aligned}
& h^{-1} [W(t+h) - W(t)] = h^{-1} \left[\sup_{0 \leqslant s \leqslant t+h} V(s) - V(t) \right] \\
= & h^{-1} \left[\max \left\{ V(t), \sup_{t \leq s \leq t+h} V(s) \right\} - V(t) \right] \leq h^{-1} \left| \sup_{t \leq s \leq t+h} V(s) - V(t) \right| \\
\leq & h^{-1} \sup_{t \leqslant s \leqslant t+h} |V(s) - V(t)| = \sup_{0 \leqslant h_0 \leqslant h} \frac{h_0}{h} h_0^{-1} |V(t+h_0) - V(t)| \\
\leqslant & \sup_{0 \leqslant h_0 \leqslant h} h_0^{-1} |V(t+h_0) - V(t)|
\end{aligned}
$$

For each $h_0 \in [0,h]$, we estimate

$$
\begin{aligned}
& h_0^{-1}\left[V\left(t+h_0\right)-V\left(t\right)\right] \\
=& h_0^{-1}\int_{-t-h_0}^{-t}\left|l\left(t+h_0\right)\left(t+h_0+c\right)-\hat{l}\left(t+h_0\right)\left(t+h_0+c\right)\right|dc \\
&+h_0^{-1}\int_{-t}^{M-t-h_0}\left|l\left(t+h_0\right)\left(t+h_0+c\right)-\hat{l}\left(t+h_0\right)\left(t+h_0+c\right)\right|dc \\
&-h_0^{-1}\int_{-t}^{M-t}\left|l\left(t\right)\left(t+c\right)-\hat{l}\left(t\right)\left(t+c\right)\right|dc \\
\leqslant& h_0^{-1}\int_0^{h_0}\left|l\left(t+h_0\right)\left(a\right)-\left(F\left(l\right)\right)\left(t\right)\right|da \\
&+h_0^{-1}\int_0^{h_0}\left|\left(F\left(l\right)\right)\left(t\right)-\left(F\left(\hat{l}\right)\right)\left(t\right)\right|da \\
&+h_0^{-1}\int_0^{h_0}\left|\left(F\left(\hat{l}\right)\right)\left(t\right)-\hat{l}\left(t+h_0\right)\left(a\right)\right|da \\
&+\int_0^{M}\left|h_0^{-1}\left[l\left(t+h_0\right)\left(a+h_0\right)-l\left(t\right)\left(a\right)\right]-G\left(l\left(t\right)\right)\left(a\right)\right|da \\
&+\int_0^{M}\left|G\left(l\left(t\right)\right)\left(a\right)-G\left(\hat{l}\left(t\right)\right)\left(a\right)\right|da \\
&+\int_0^{M}\left|h_0^{-1}\left[\hat{l}\left(t+h_0\right)\left(a+h_0\right)-\hat{l}\left(t\right)\left(a\right)\right]-G\left(\hat{l}\left(t\right)\right)\left(a\right)\right|da
\end{aligned}
$$

So for both of the above situations, notice that both l and $\hat{l}$ are solutions of problem (III.4), we can estimate as the following:

$$
\begin{aligned}
& \limsup_{h\to 0^+} h^{-1}\left[W\left(t+h\right)-W\left(t\right)\right] \leqslant \limsup_{h\to 0^+}\sup_{0\leqslant h_0\leqslant h} h_0^{-1}\left|V\left(t+h_0\right)-V\left(t\right)\right| \\
\leqslant& \left|\left(F\left(l\right)\right)\left(t\right)-\left(F\left(\hat{l}\right)\right)\left(t\right)\right|+\left\|G\left(l\left(t\right)\right)-G\left(\hat{l}\left(t\right)\right)\right\|_{L^1} \\
\leqslant& c_2\left(r,t\right)\sup_{0\leqslant s\leqslant t}\left\|l\left(s\right)-\hat{l}\left(s\right)\right\|_{L^1}+c_1\left(r\right)\left\|l\left(t\right)-\hat{l}\left(t\right)\right\|_{L^1} \\
\leqslant& \left[c_1\left(r\right)+c_2\left(r,T\right)\right]W\left(t\right)
\end{aligned}
$$

So we have $W(t) \leqslant e^{[c_1(r)+c_2(r,T)]t} W(0)$ (Lakshmikantham and Leela (1969), Theorem 1.4.1). Hence,

$$V(t) \leqslant W(t) \leqslant e^{[c_1(r)+c_2(r,T)]t} W(0) = e^{[c_1(r)+c_2(r,T)]t} \left\| \phi - \hat{\phi} \right\|_{L^1}$$

That is,

$$\left\| l(t) - \hat{l}(t) \right\|_{L^1} \leqslant e^{[c_1(r)+c_2(r,T)]t} \left\| \phi - \hat{\phi} \right\|_{L^1}$$

□

VII.2 Theorem III.4.3 and Theorem III.4.4

Proof of Theorem III.4.3 and Theorem III.4.4. The proof of Theorem III.4.3 and Theorem III.4.4 are similar to that of the corresponding theorems in Sections $2.3-2.4$ in Webb (1985). We only need to switch the statement of Proposition 2.4 in Webb (1985) to the following Proposition VII.2.1. □

Proposition VII.2.1. *Let (H.1), (H.2) hold, let $\phi \in L^1$, let $T > 0$, and let $l \in C_T$ such that l is a solution of* (VII.1) *on $[0,T]$. Let $\hat{T} > 0$ and let $\hat{l} \in C_{T+T}$ such that $\hat{l}(t) = l(t)$ for $t \in [0,T]$, and for $t \in \left(T, T+\hat{T}\right]$, $\hat{l}$ satisfies the following integral equation:*

$$\hat{l}(t)(a) = \begin{cases} \left(F\left(\hat{l}\right)\right)(t-a) + \int_{t-a}^{t} G\left(\hat{l}(s)\right)(s+a-t)\,ds, & 0 < a < t-T \\ l(T)(a-t+T) + \int_{T}^{t} G\left(\hat{l}(s)\right)(s+a-t)\,ds, & t-T \leqslant a \leqslant \mathrm{M} \end{cases}$$

Then $\hat{l}$ is a solution of (VII.1) *on $\left[0, T+\hat{T}\right]$.*

Proof. First of all, we notice that if $(H.2)$ holds, then $(F(l))(t) = \left(F\left(\hat{l}\right)\right)(t)$ for $t \in$

$[0,T]$. Because for any $t \in [0,T]$, by $(H.2)$, $\exists C > 0$ such that

$$\left|\left(F\left(l\right)\right)\left(t\right) - \left(F\left(\hat{l}\right)\right)\left(t\right)\right| \leqslant C \sup_{0\leqslant s\leqslant t} \left\|l\left(s\right) - \hat{l}\left(s\right)\right\|_{L^1} = 0$$

Then it is easy to verify that $\hat{l}$ is a solution to (VII.1) for $t \in [0,T]$. Next, we verify that $\hat{l}$ is a solution to (VII.1) for $t \in \left(T, T+\hat{T}\right]$.

For $t - T \leqslant a \leqslant M$:

1. If $a \geqslant t$,

$$\begin{aligned}
&\hat{l}\left(t\right)\left(a\right) = l\left(T\right)\left(a-t+T\right) + \int_T^t G\left(\hat{l}\left(s\right)\right)\left(s+a-t\right)ds \\
&= \left(F\left(l\right)\right)\left(t-a\right) + \int_{t-a}^T G\left(l\left(s\right)\right)\left(s+a-t\right)ds + \int_T^t G\left(\hat{l}\left(s\right)\right)\left(s+a-t\right)ds \\
&= \left(F\left(\hat{l}\right)\right)\left(t-a\right) + \int_{t-a}^t G\left(\hat{l}\left(s\right)\right)\left(s+a-t\right)ds
\end{aligned}$$

2. If $a < t$,

$$\begin{aligned}
&\hat{l}\left(t\right)\left(a\right) = l\left(T\right)\left(a-t+T\right) + \int_T^t G\left(\hat{l}\left(s\right)\right)\left(s+a-t\right)ds \\
&= \phi\left(a-t\right) + \int_0^T G\left(l\left(s\right)\right)\left(s+a-t\right)ds + \int_T^t G\left(\hat{l}\left(s\right)\right)\left(s+a-t\right)ds \\
&= \phi\left(a-t\right) + \int_0^t G\left(\hat{l}\left(s\right)\right)\left(s+a-t\right)ds
\end{aligned}$$

For $0 \leqslant a \leqslant t - T$, the verification is straightforward. □

VII.3 Theorem IV.1.1

Proof of Theorem IV.1.1. By Theorem III.4.3 and Theorem III.4.4, We only need to show that the aging function G in $(P.1)$ and the birth function F in $(P.2)$ satisfy the hypotheses

$(H.1)-(H.5)$. $(H.3)$ and $(H.4)$ are obvious from $(P.1)$ and $(P.2)$, we will justify $(H.1)$ and $(H.2)$ as follows. First denote $\bar{\mu} := \|\mu\|_{L^\infty}$. Let $r > 0$, for any ϕ_1, $\phi_2 \in L^1$ such that $\|\phi_1\|_{L^1}$, $\|\phi_2\|_{L^1} \leq r$, we have

$$\begin{aligned}
&\|G(\phi_1) - G(\phi_2)\|_{L^1} \\
\leqslant &\int_0^M \mu(a) |\phi_1(a) - \phi_2(a)| \, da + \mathcal{T}(\phi_1) \int_0^M |\phi_1(a) - \phi_2(a)| \, da \\
&+ |\mathcal{T}(\phi_1) - \mathcal{T}(\phi_2)| \int_0^M |\phi_2(a)| \, da \\
\leqslant &(\bar{\mu} + 2r\|\mathcal{T}\|_\infty) \|\phi_1 - \phi_2\|_{L^1}
\end{aligned}$$

so we have $(H.1)$. In order to prove $(H.2)$, first we notice that $t \mapsto (F(\phi))(t)$ is continuous in $[0, \infty)$ for any $\phi \in C_T$. So $F : C_T \to C([0,T]; \mathbb{R})$.

Next, for any ϕ_1, $\phi_2 \in C_T$ such that $\|\phi_1\|_{C_T}$, $\|\phi_2\|_{C_T} \leq r$, we have $\forall t \in [0,T]$,

$$\begin{aligned}
&|(F(\phi_1))(t) - (F(\phi_2))(t)| \\
\leq &S_0 |\mathcal{B}(\phi_1(t)) - \mathcal{B}(\phi_2(t))| \, e^{-\int_0^t \mathcal{B}(\phi_1(s)) + \mathcal{Q}(\phi_1(s)) ds} \\
&+ S_0 \mathcal{B}(\phi_2(t)) \left| e^{-\int_0^t \mathcal{B}(\phi_1(s)) + \mathcal{Q}(\phi_1(s)) ds} - e^{-\int_0^t \mathcal{B}(\phi_2(s)) + \mathcal{Q}(\phi_2(s)) ds} \right| \\
= &: I_1 + I_2
\end{aligned}$$

Obviously, $I_1 \leq S_0 |\mathcal{B}| \|\phi_1(t) - \phi_2(t)\|_{L^1} e^{rt(|\mathcal{Q}| + |\mathcal{B}|)}$.

In order to consider I_2, notice that $\left|e^X - e^Y\right| \leq e^M |X - Y|$ for $|X|$, $|Y| \leq M$. Then we have

$$\begin{aligned}
I_2 \leqslant &S_0 |\mathcal{B}| r e^{rt(|\mathcal{Q}| + |\mathcal{B}|)} \int_0^t |\mathcal{B}(\phi_1(s)) + \mathcal{Q}(\phi_1(s)) - \mathcal{B}(\phi_2(s)) - \mathcal{Q}(\phi_2(s))| \, ds \\
\leq &S_0 |\mathcal{B}| r e^{rt(|\mathcal{Q}| + |\mathcal{B}|)} (|\mathcal{B}| + |\mathcal{Q}|) \int_0^t \|\phi_1(s) - \phi_2(s)\|_{L^1} ds
\end{aligned}$$

Hence,

$$\begin{aligned}&|(F(\phi_1))(t)-(F(\phi_2))(t)|\\ \leq& S_0|\mathcal{B}|e^{rt(|\mathcal{Q}|+|\mathcal{B}|)}\left[1+rt(|\mathcal{B}|+|\mathcal{Q}|)\right]\sup_{0\leqslant s\leqslant t}\|\phi_1(s)-\phi_2(s)\|_{L^1}\end{aligned}$$

Now we let $l\in C\left([0,T_\phi);L^1_+\right)$ be the positive solution of (III.4), then for any $t\in[0,T_\phi)$, $(H.5)$ is easy to verify:

$$(F(l))(t)+\int_0^M G(l(t))(a)\,da\leqslant S_0|\mathcal{B}|\int_0^M l(t)(a)\,da$$

So by Theorem III.4.4, there is a positive global solution of (III.4). □

VII.4 Proposition IV.2.1

Proof of Proposition IV.2.1. Proof of the existence of the global positive solution is based on the following four lemmas. An easy computation can be done to testify that a solution of (IV.1) is also a solution in the sense of (III.4) with aging function $\mathcal{P}$ and birth function $\mathcal{H}$. □

Lemma VII.4.1. *Let the assumptions in Proposition IV.2.1 hold, and let $r>0$. There exists $T>0$ such that if $\|\phi\|_{L^1}\leqslant r$, then there is a unique function $u\in C_{T,+}$ such that u is a solution of* (IV.1) *on* $[0,T]$.

Proof. We can choose a sufficiently small $T>0$ and define

$$S:=\left\{u\in C_{T,+}:u(t)=\phi,\|u\|_{C_T}\leqslant 2r\right\}$$

An argument which is similar to that of Proposition VII.1.2 can be used to show that a

mapping defined by (IV.1) from S into S is a strict contraction. Thus, the unique fixed point is a positive solution of (IV.1) in $C_{T,+}$. □

Lemma VII.4.2. *Let the assumptions in Proposition IV.2.1 hold, let $T > 0$, and let $u \in C_{T,+}$ such that u is a solution of* (IV.1) *on $[0,T]$. Let $\hat{T} > 0$ and let $\hat{u} \in C_{T+\hat{T},+}$ such that $\hat{u}(t) = u(t)$ for $t \in [0,T]$, and for $t \in \left(T, T+\hat{T}\right]$, $\hat{u}$ satisfies the integral equation:*

$$\hat{u}(t)(a) = \begin{cases} (\mathcal{H}(\hat{u}))(t-a)\, e^{-\int_0^a \mu(b)db}, \ 0 < a < t-T \\ u(T)(a-t+T)\, e^{-\int_{a-t+T}^a \mu(b)db}, \ t-T \leq a \leq \mathrm{M} \end{cases}$$

where $\mathcal{H}$ is as stated in Proposition IV.2.1. Then $\hat{u}$ is a solution of (IV.1) *on $\left[0, T+\hat{T}\right]$.*

Proof. The proof is similar to that of Proposition VII.2.1. □

Lemma VII.4.3. *Let the assumptions in Proposition IV.2.1 hold, let $\phi \in L^1_+$, and let u be the solution of* (IV.1) *on its maximal interval of existence $[0, T_\phi)$. If $T_\phi < \infty$, then* $\limsup_{t \to T_\phi^-} \|u(t)\|_{L^1} = \infty$.

Proof. The proof is similar to that of Theorem 2.3 in Webb (1985). □

Lemma VII.4.4. *Let the assumptions in Proposition IV.2.1 hold, let $\phi \in L^1_+$, and let u be the positive solution of* (IV.1) *on its maximal interval of existence $[0, T_\phi)$. Then $\exists \omega \in \mathbb{R}$, and for $t \in [0, T_\phi)$, $\|u(t)\|_{L^1} \leqslant \|\phi\|_{L^1} e^{\omega t}$. So $T_\phi = \infty$, there is a global positive solution of* (IV.1).

Proof. For $t \in [0, T_\phi)$, we estimate as follows (here we assume $t \leqslant M$, then $t > M$ leads

to a simpler case):

$$\begin{aligned}
&\|u(t)\|_{L^1} = \int_0^M u(t)(a)\,da \leqslant \int_0^t (\mathcal{H}(u))(t-a)\,da + \int_t^M \phi(a-t)\,da \\
\leqslant &\int_0^t S_0 |\mathcal{B}| \|u(t-a)\|_{L^1} da + \int_t^M \phi(a-t)\,da \\
\leqslant &S_0 |\mathcal{B}| \int_0^t \|u(s)\|_{L^1} ds + \int_0^{M-t} \phi(s)\,ds \\
\leqslant &S_0 |\mathcal{B}| \int_0^t \|u(s)\|_{L^1} ds + \|\phi\|_{L^1}
\end{aligned}$$

Then by Gronwall's Inequality, we have $\|u(t)\|_{L^1} \leqslant \|\phi\|_{L^1} e^{S_0|\mathcal{B}|t}$. Then by Lemma VII.4.3, $T_\phi = \infty$, hence there is a positive global solution to (IV.1). □

VII.5 Theorem IV.3.1

Proof of Theorem IV.3.1. Let $T > 0$, we assume that $u \in C\left([0,T]; L^1_+\right)$ satisfies (IV.1) for $t \in [0,T]$, then u satisfies the following conditions:

$$\begin{aligned}
&\lim_{h\to 0^+} \int_0^M \left| h^{-1}\left[u(t+h)(a+h) - u(t)(a)\right] + \mu(a)\,u(t)(a) \right| da = 0 \\
&\lim_{h\to 0^+} h^{-1} \int_0^h \left| u(t+h)(a) - (\mathcal{H}(u))(t) \right| da = 0 \\
&u(0) = \phi
\end{aligned} \tag{VII.2}$$

We will show that $l \in C\left([0,T]; L^1_+\right)$ as obtained from (IV.2), satisfies (III.4) with the aging function G in (P.1) and the birth function F in (P.2). For the first condition in

(III.4), we have the following estimation:

$$
\begin{aligned}
& h^{-1}\left[l\left(t+h\right)\left(a+h\right)-l\left(t\right)\left(a\right)\right]+\mu\left(a\right)l\left(t\right)\left(a\right)+\mathcal{T}\left(l\left(t\right)\right)l\left(t\right)\left(a\right)\\
=&\frac{h^{-1}\left[u\left(t+h\right)\left(a+h\right)-u\left(t\right)\left(a\right)\right]+\mu\left(a\right)u\left(t\right)\left(a\right)}{1+\int_0^{t+h}\mathcal{T}\left(u\left(s\right)\right)ds}\\
&+\left[\frac{\mu\left(a\right)u\left(t\right)\left(a\right)}{1+\int_0^{t}\mathcal{T}\left(u\left(s\right)\right)ds}-\frac{\mu\left(a\right)u\left(t\right)\left(a\right)}{1+\int_0^{t+h}\mathcal{T}\left(u\left(s\right)\right)ds}\right]\\
&+h^{-1}\left[\frac{u\left(t\right)\left(a\right)}{1+\int_0^{t+h}\mathcal{T}\left(u\left(s\right)\right)ds}-\frac{u\left(t\right)\left(a\right)}{1+\int_0^{t}\mathcal{T}\left(u\left(s\right)\right)ds}\right]+\frac{\mathcal{T}\left(u\left(t\right)\right)u\left(t\right)\left(a\right)}{\left(1+\int_0^{t}\mathcal{T}\left(u\left(s\right)\right)ds\right)^2}\\
:=&I_1+I_2+I_3
\end{aligned}
$$

By (VII.2), $I_1\to 0$ as $h\to 0$. $I_2\to 0$ as $h\to 0$ because of the absolute continuity of Lebesgue integral. If we compute the derivative of function $f\left(t\right):=\frac{1}{1+\int_0^t\mathcal{T}(u(s))ds}$, we get $I_3\to 0$ as $h\to 0$. Hence the first limit in the solution definition (III.4) is satisfied. For the second condition in (III.4), we have

$$
\begin{aligned}
&\int_0^h\left|l\left(t+h\right)\left(a\right)-\left(F\left(l\right)\right)\left(t\right)\right|da\\
=&\int_0^h\left|l\left(t+h\right)\left(a\right)-S_0\mathcal{B}\left(l\left(t\right)\right)e^{-\int_0^t\mathcal{B}(l(s))+\mathcal{Q}(l(s))ds}\right|da\\
=&\int_0^h\left|\frac{u\left(t+h\right)\left(a\right)-\left(\mathcal{H}\left(u\right)\right)\left(t\right)}{1+\int_0^t\mathcal{T}\left(u\left(s\right)\right)ds}\right|da\to 0,\ \left(h\to 0^+\right)
\end{aligned}
$$

The third condition in (III.4) is straightforward. Then by Proposition IV.2.1, we can find a $u\in C\left(\left[0,\infty\right);L^1_+\right)$ that satisfies (IV.1). Then a positive global solution to problem (III.4) can be obtained by (IV.2), which is exactly the unique positive global solution to (III.4). □

VII.6 Theorem IV.4.1

Proof of Theorem IV.4.1. Let $u \in C\left([0,\infty);L^1_+\right)$ be the solution to (IV.1), and let $i \in C\left([0,\infty);L^1_+\right)$ as defined in (IV.2), which is a solution to problem (III.1) in the sense of (III.4). For convenience in this proof, we use the notation $i(a,t) := i(t)(a)$ and $u(a,t) := u(t)(a)$, for $a \in [0,M]$, $t \in [0,\infty)$. Firstly, by (III.1) we have

$$S(t) = S_0 e^{-\int_0^t \mathcal{B}(i(\cdot,s))+\mathcal{Q}(i(\cdot,s))ds}$$

which is a positive non-increasing continuous function of $t \in [0,\infty)$. So $\lim_{t\to\infty} S(t)$ exists, and we denote it as $\lim_{t\to\infty} S(t) = S_\infty \geqslant 0$. Next we estimate the following:

$$\begin{aligned}
&\int_0^\infty \mathcal{B}(i(\cdot,t)) + \mathcal{Q}(i(\cdot,t))\,dt \leqslant \int_0^\infty (|\mathcal{B}|+|\mathcal{Q}|)\,\|i(\cdot,t)\|_{L^1} dt \\
=&(|\mathcal{B}|+|\mathcal{Q}|)\int_0^\infty\int_0^M \frac{u(a,t)}{1+\int_0^t \mathcal{T}(u(\cdot,s))\,ds} da dt \\
=&(|\mathcal{B}|+|\mathcal{Q}|)\int_0^M\int_0^a \frac{\phi(a-t)\,e^{-\int_{a-t}^a \mu(b)db}}{1+\int_0^t \mathcal{T}(u(\cdot,s))\,ds} dt da \\
&+(|\mathcal{B}|+|\mathcal{Q}|)\int_0^M\int_a^\infty \frac{u(0,t-a)\,e^{-\int_0^a \mu(b)db}}{1+\int_0^t \mathcal{T}(u(\cdot,s))\,ds} dt da \\
:=&(|\mathcal{B}|+|\mathcal{Q}|)(I_1+I_2)
\end{aligned}$$

Estimate I_1 and I_2 separately:

$$
\begin{aligned}
I_1 \leqslant & \int_0^M \int_0^a \phi(a-t) e^{-\int_{a-t}^a \mu(b)db} dtda = \int_0^M \int_0^a \phi(s) e^{-\int_s^a \mu(b)db} dsda \\
= & \int_0^{a_0} \int_0^a \phi(s) e^{-\int_s^a \mu(b)db} dsda + \int_{a_0}^M \int_0^a \phi(s) e^{-\int_s^a \mu(b)db} dsda \\
\leqslant & \int_0^{a_0} \int_0^a \phi(s) dsda + \int_{a_0}^M \int_0^a \phi(s) e^{-\mu_0(a-s)} dsda \\
\leqslant & a_0 \|\phi\|_{L^1} + \int_0^M \int_0^a \phi(s) e^{-\mu_0(a-s)} dsda \\
= & a_0 \|\phi\|_{L^1} + \int_0^M \int_s^M \phi(s) e^{-\mu_0(a-s)} dads \\
= & a_0 \|\phi\|_{L^1} + \int_0^M \int_0^{M-s} \phi(s) e^{-\mu_0\tau} d\tau ds \\
\leqslant & a_0 \|\phi\|_{L^1} + \int_0^M \int_0^M \phi(s) e^{-\mu_0\tau} d\tau ds \\
= & a_0 \|\phi\|_{L^1} + \left(\int_0^M e^{-\mu_0\tau} d\tau \right) \|\phi\|_{L^1} < \infty
\end{aligned}
$$

$$
\begin{aligned}
I_2 = & \int_0^M \int_a^\infty \frac{u(0, t-a) e^{-\int_0^a \mu(b)db}}{1 + \int_0^t \mathcal{T}(u(\cdot, s)) ds} dtda \\
\leqslant & \int_0^M \int_0^\infty \frac{u(0,\tau) e^{-\int_0^a \mu(b)db}}{1 + \int_0^{a+\tau} \mathcal{T}(u(\cdot, s)) ds} d\tau da \\
\leqslant & \int_0^M \int_0^\infty \frac{u(0,\tau) e^{-\int_0^a \mu(b)db}}{1 + \int_0^\tau \mathcal{T}(u(\cdot, s)) ds} d\tau da \\
= & \left(\int_0^\infty i(0,\tau) d\tau \right) \left(\int_0^M e^{-\int_0^a \mu(b)db} da \right) \\
\leqslant & \left(\int_0^\infty i(0,\tau) d\tau \right) \left(a_0 + \int_{a_0}^M e^{-a\mu_0} da \right)
\end{aligned}
$$

With the assumption on function μ, we can find constants C_1, $C_2 > 0$ such that:

$$
\int_0^\infty \mathcal{B}(i(\cdot, t)) + \mathcal{Q}(i(\cdot, t)) dt \leqslant C_1 + C_2 \int_0^\infty i(0,t) dt
$$

Since i is obtained from (IV.2), we have:

$$i\left(0,t\right)=\frac{u\left(0,t\right)}{1+\int_{0}^{t}\mathcal{T}\left(u\left(\cdot,s\right)\right)ds}=S\left(t\right)\mathcal{B}\left(i\left(\cdot,t\right)\right)$$

Then by the differential equation of $S(t)$ in (III.1), we have:

$$i\left(0,t\right)=-\frac{dS\left(t\right)}{dt}-\mathcal{Q}\left(i\left(\cdot,t\right)\right)S\left(t\right)\leqslant-\frac{dS\left(t\right)}{dt}$$

Integrate on both sides with respect to t of the above inequality,

$$\int_{0}^{\infty}i\left(0,t\right)dt\leqslant S_{0}-S_{\infty}<\infty$$

Hence one of the conclusion is proved:

$$\lim_{t\to\infty}S\left(t\right)=S_{0}e^{-\int_{0}^{\infty}\mathcal{B}(i(\cdot,s))+\mathcal{Q}(i(\cdot,s))ds}\geqslant S_{0}e^{-C_{1}-C_{2}\int_{0}^{\infty}i(0,t)dt}>0$$

Moreover, it can be derived from the differential equation system (III.1) that:

$$\begin{aligned}&S\left(t\right)+I\left(t\right)+\int_{0}^{t}\mathcal{Q}\left(i\left(\cdot,s\right)\right)I\left(s\right)ds+\int_{0}^{t}\mathcal{T}\left(i\left(\cdot,s\right)\right)I\left(s\right)ds+\int_{0}^{t}i\left(M,s\right)ds\\&+\int_{0}^{t}\int_{0}^{M}\mu\left(a\right)i\left(a,s\right)dads=S_{0}+I\left(0\right)\end{aligned}\tag{VII.3}$$

where the four integrals in (VII.3) are non-decreasing with respect to the variable t and have $S_0 + I(0)$ as an upper bound. So the four integrals all have finite limit as $t \to \infty$. Then the fact that $\lim_{t\to\infty} S(t)$ exists implies that $\lim_{t\to\infty} I(t)$ exists. We can estimate $\int_0^\infty I(t)\,dt = \int_0^\infty \|i(t)\|_{L^1} dt$ similarly as we did in the beginning of this proof and get $\int_0^\infty I(t)\,dt < \infty$, which implies the conclusion $\lim_{t\to\infty} I(t) = 0$.

□

BIBLIOGRAPHY

Aldis G, Roberts M (2005) An integral equation model for the control of a smallpox outbreak. Math Biosci 195(1):1–22, DOI 10.1016/j.mbs.2005.01.006

Arino J, Brauer F, van den Driessche P, Watmough J, Wu J (2006) Simple models for containment of a pandemic. J R Soc Interface 3:453–457, DOI 10.1098/rsif.2006.0112

Bauch C, Lloyd-Smith J, Coffee M, Galvani A (2005) Dynamically modeling SARS and other newly emerging respiratory illnesses, past, present, and future. Epidemiology 16(6):791–801, DOI 10.1097/01.ede.0000181633.80269.4c

Carrat F, Vergu E, Ferguson N, Lemaitre M, Cauchemez S, Leach S, Valleron AJ (2008) Time lines of infection and disease in human influenza: A review of volunteer challenge studies. Am J Epidemiol 167(7):775–785, DOI 10.1093/aje/kwm375

CDC (2003) Recommendations for using smallpox vaccine in a pre-event vaccination program. http://www.cdc.gov/mmwr/preview/mmwrhtml/rr5207a1.htm

CDC (2004) Smallpox Fact Sheet. http://www.bt.cdc.gov/agent/smallpox/overview/disease-facts.asp

Chan P, *et al* (2004) Laboratory diagnosis of SARS. Emerg Infect Dis 10(5):825–831, DOI 10.3201/eid1005.030682

CIDRAP (2002) CIA believes four nations have secret smallpox virus stocks. http://www.cidrap.umn.edu/news-perspective/2002/11/cia-believes-four-nations-have-secret-smallpox-virus-stocks-report-says

Day T, Park A, Madras N, Gumel A, Wu J (2006) When is quarantine a useful control strategy for emerging infectious diseases? Am J Epidemiol 163:479–485, DOI 10.1093/aje/kwj056

Eichner M (2003) Case isolation and contact tracing can prevent the spread of smallpox. Am J Epidemiol 158(2):118–28, DOI 10.1093/aje/kwg104

Feng Z, Xu D, Zhao H (2007) Epidemiological models with non-exponentially distributed disease stages and applications to disease control. Bull Math Bio 69:1511–1536, DOI 10.1007/s11538-006-9174-9

Feng Z, Yang Y, Xu D, Zhang P, McCauley M, Glasser J (2009) Timely indentification of optimal control strategies for emerging infectious diseases. J Theor Biol 1(259):165–71, DOI 10.1016/j.jtbi.2009.03.006

Feng Z, Towers S, Yang Y (2011) Modeling the effects of vaccination and treatment on pandemic influenza. AAPS J 13(3):427–37, DOI 10.1208/s12248-011-9284-7

Fraser C, Riley S, Anderson R, Ferguson N (2004) Factors that make an infectious disease outbreak controllable. Proc Natl Acad Sci USA 101(16):6146–51, DOI 10.1073/pnas.0307506101

Glasser J, Hupert N, McCauley M, Hatchett R (2011) Modeling and public health emergency responses: Lessons from SARS. Epidemics 1(3):32–7, DOI 10.1016/j.epidem.2011.01.001

Gumel A, Ruan S, Day T, Watmough J, Brauer F, van den Driessche P, Gabrielson D, Bowman C, Alexander M, Ardal S, Wu J, Sahai B (2004) Modelling strategies for controlling SARS outbreaks. Proc Biol Sci 271(1554):2223–32, DOI 10.1098/rspb.2004.2800

Halloran M, Jr IL, Nizam A, Yang Y (2002) Containing bioterrorist smallpox. Sci Mag 298:1428, DOI 10.1126/science.1074674

Hansen S, *et al* (2013) Immune clearance of highly pathogenic SIV infection. Nature Published online, 11 September, DOI 10.1038/nature12519

Hethcote H, Ma Z, Liao S (2002) Effects of quarantine in six endemic models for infectious diseases. Math Biosci 180:141–160, DOI 10.1016/S0025-5564(02)00111-6

Hsieh Y, Chen W, Hsu S (2004) SARS Outbreak, Taiwan, 2003. Emerg Infect Dis 10(2):201–206, DOI 10.3201/eid1002.030515

Hsu L, *et al* (2003) Severe Acute Respiratory Syndrome (SARS) in singapore: clinical features of index patient and initial contacts. Emerg Infect Dis 9(6):713–717, DOI 10.3201/eid0906.030264

Hsu SB, Hsieh YH (2006) Modeling intervention measures and severity-dependent public response during Severe Acute Respiratory Syndrome outbreak. SIAM J Appl Math 66(2):627–647, DOI 10.1137/040615547

Inaba H, Nishiura H (2008) The state-reproduction number for a multistate class age structured epidemic system and its application to the asymptomatic transmission model. Math Biosci 216(1):77–89, DOI 10.1016/j.mbs.2008.08.005

Kaplan E, Craft D, Wein L (2002) Emergency response to a smallpox attack: The case for mass vaccination. Proc Natl Acad Sci USA 99(16):10,935–10,940, DOI 10.1073/pnas.162282799

Kaplan E, Craft D, Wein L (2003) Analyzing bioterror response logistics: the case of smallpox. Math Biosci 185(1):33–72, DOI 10.1016/S0025-5564(03)00090-7

Kretzschmar M, van den Hof S, Wallinga J, van Wijngaarden J (2004) Ring vaccination and smallpox control. Emerg Infect Dis 10(5):832–841, DOI 10.3201/eid105.030419

Lakshmikantham V, Leela S (1969) Differential and Integral Inequalities. Academic Press

Meltzer M (2004) Multiple contact dates and SARS incubation periods. Emerg Infect Dis 10(2):207–209, DOI 10.3201/eid1002.030426

Meltzer M, Damon I, LeDuc J, Millar J (2001) Modeling potential responses to smallpox as a bioterrorist weapon. Emerg Infect Dis 7(6):959–69, DOI 10.321/eid0706.0607

MMWR (2003) Use of Quarantine to Prevent Transmission of Severe Acute Respiratory Syndrome-Taiwan, 2003. http://www.cdc.gov/mmwr/preview/mmwrhtml/mm5229a2.htm

Müller J, Kretzschmar M, Dietz K (2000) Contact tracing in stochastic and deterministic epidemic models. Math Biosci 164(1):39–64, DOI 10.1016/S0025-5564(99)00061-9

NewYorkTimes (2013) Wary of Attack with Smallpox, U.S. buys up a costly drug. http://www.nytimes.com/2013/03/13/health/us-stockpiles-smallpox-drug-in-case-of-bioterror-attack.html

Nishiura H, Patanarapelert K, Sriprom M, Sarakorn W, Sriyab S, Tang IM (2004) Modelling potential responses to severe acute respiratory syndrome in Japan: the role of initial attack size, precaution, and quarantine. J Epidemiol Community Health 227:369–379, DOI 10.1136/jech.2003.014894

Peiris J, *et al* (2003) Clinical progression and viral load in a community outbreak of coronavirus-associated SARS pneumonia: a prospective study. Lancet 361(9371):1767–72, DOI 10.1016/S0140-6736(03)13412-5

Valle SD, Hethcote H, Hyman J, Castillo-Chavez C (2005) Effects of behavioral changes in a smallpox attack model. Math Biosci 195(2):228–251, DOI 10.1016/j.mbs.2005.03.006

Vidondo B, Schwehm M, Bühlmann A, Eichner M (2012) Finding and removing highly connected individuals using suboptimal vaccines. BMC Infect Dis 12(51), DOI 10.1186/1471-2334-12-51

Wang W, Ruan S (2003) Simulating the SARS outbreak in Beijing with limited data. J Theor Biol 58:186–191, DOI 10.1016/j.jtbi.2003.11.014

Webb G (1985) Theory of Nonlinear Age-dependent Population Dynamics. Chapman & Hall Pure and Applied Mathematics

Webb G, Hsieh YH, Wu J, Blaser M (2010) Pre-symptomatic Influenza Transmission, Surveillance, and School Closings: Implications for Novel Influenza A (H1N1). Math Model Nat Phenom 5(3):191–205, DOI 10.1051/mmnp/20105312